

Search JNP

 [RSS feed for the Journal of Nanophotonics](#)

[Advanced Search](#)
[J. Nanophoton.](#) / [Volume 2](#) / [Issue 1](#) / [Special Section on Nanophotonics in Europe](#)
 [PRINT PAGE](#)

Photonic energy lifters and event horizons with time-dependent dielectric structures

J. Nanophoton., Vol. 2, 021853 (2008); DOI:10.1117/1.3054303

Published 2 December 2008

Zeno Gaburro

Dipartimento di Fisica, Universita degli Studi di Trento, via Sommarive 14, Povo, Trento 38100 Italy

Novel photonic devices, based on time-dependent dielectrics, to shift the optical frequency, may be conceived from two complementary principles, Doppler shift and time refraction, and possibly realized as as single cavities or as Coupled Resonator Optical Waveguides (CROWs). Simulations with the finite-difference time-domain method bore out these possibilities and also provided design rules. Preliminary experiments, limited to a pulsed excitation (without any frequency shift) of whispering gallery modes in a LiNbO_3 whispering gallery disk resonator in a full fiber-optics setup, the first experiments of an optical whispering-gallery resonator functioning in the steady-pulsed regime, led to a consistent Q-factor measurement between CW and pulsed ringdown characterization. The repetition rate was tuned to an integer submultiple $1/N$ of the free spectral range of the resonator. The output rate of the resonator was equal to the input rate multiplied by N , thereby showing functionality as a frequency multiplier. The impact of nonlinearity and of dispersion was minimized by the low power level and the limited bandwidth of pulses.

©2008 *Society of Photo-Optical Instrumentation Engineers*

History: Received 4 August 2008; revised 24 November 2008; accepted 25 November 2008; published 2 December 2008

DOI Link: <http://dx.doi.org/10.1117/1.3054303>

JOURNAL DATA

ISSN:

1934-2608 (print) 1934-2608 (online)

Publisher:

SPIE



REFERENCES (107)

For access to fully linked references, you need to [Log in](#).

CITING ARTICLES

For access to citing articles, you need to [Log in](#).

[home](#) | [proceedings](#) | [journals](#)

[Terms of Use](#) | [Privacy Policy](#) | [Contact](#)



SPIE © 1990 – 2008

Photonic energy lifters and event horizons with time-dependent dielectric structures

Z. Gaburro

Dipartimento di Fisica, Università degli Studi di Trento,
via Sommarive, 14 - 38100 Trento, Italy.
gaburro@science.unitn.it

Abstract. Novel photonic devices, based on time-dependent dielectrics, to shift the optical frequency, may be conceived from two complementary principles, Doppler shift and time refraction, and possibly realized as single cavities or as Coupled Resonator Optical Waveguides (CROWs). Simulations with the finite-difference time-domain method bore out these possibilities and also provided design rules. Preliminary experiments, limited to a pulsed excitation (without any frequency shift) of whispering gallery modes in a LiNbO_3 whispering gallery disk resonator in a full fiber-optics setup, the first experiments of an optical whispering-gallery resonator functioning in the steady-pulsed regime, led to a consistent Q -factor measurement between CW and pulsed ringdown characterization. The repetition rate was tuned to an integer submultiple $1/N$ of the free spectral range of the resonator. The output rate of the resonator was equal to the input rate multiplied by N , thereby showing functionality as a frequency multiplier. The impact of nonlinearity and of dispersion was minimized by the low power level and the limited bandwidth of pulses.

Keywords: Doppler effect, coupled resonators, whispering gallery resonator, lithium niobate.

1 INTRODUCTION

Because of its implications on the formulation of a consistent quantum theory of gravity, there is a great deal of interest in looking for experimental tests of Hawking's arguments about black hole radiation [1]. Experimental tests on astronomic black holes are very difficult to be imagined because the expected Hawking radiation is extremely weak compared to cosmic radiation background, thus a significant amount of research has devoted to create lab-based black-hole analogous, following an original proposal by Unruh [2], by generating the equivalent of a gravitational event horizon for light or for sonic waves [3–18].

Yablonovitch has proposed a way to achieve moving interfaces in optically nonlinear media [19,20]. The intriguing feature of this proposal is that it deals with *moving* optical interfaces in *still* media: since there is no real mechanical motion, it becomes feasible in such scheme to conceive “motions” of these interfaces which approach or even exceed the phase speed of light in the medium in which the interface is generated. Hence, it is a very promising approach towards the demonstration of event horizons. Figure 1 illustrates, in principle, a way to realize an event horizon for light with a moving interface between two media, each exhibiting a different velocity of propagation for light. A device behaving as in Fig. 1 has been recently demonstrated in a fiber optics setup [21,22]. Even though I am not going into this topic here, possible implementations of devices generating the effect described in Fig. 1 are certainly of great interest. Beside their use for the study of Unruh effect, one might wonder whether such devices can be interesting also for other applications. The effect described in Fig. 1 is a particular case (in the sense that the motion of the interface is restricted to $v_{slow} < v_{interf} < v_{fast}$) of a generalized *refraction* of the wave. The generalization I am referring to derives from the motion of the interface: in fact, the well known textbook treatment of refraction is time-independent, the interface being still ($v_{interf} = 0$). The interaction of electromagnetic waves with moving interfaces

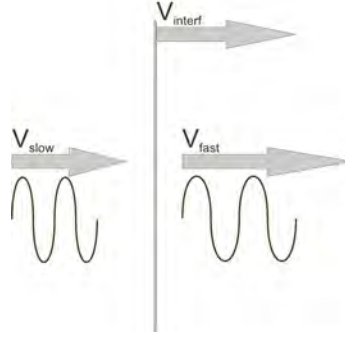


Fig. 1. A moving interface with velocity v_{interf} between media characterized by low and high phase velocity (v_{slow} and v_{fast}) of a wave behaves as an event horizon for this wave, emulating the event horizon of a gravitational black hole, if $v_{slow} < v_{interf} < v_{fast}$. In fact, the wave ahead of the interface can escape but the one behind cannot. If the direction of all the velocities is flipped (i.e. time is reversed), the interface emulates a white-hole horizon.

has been extensively studied, both in the case of mechanical [23–29] and non-mechanical motions, the latter being originated by modulation of the optical response of an immobile medium [30–35]. The quantitative analysis of the time-independent case reveals that one must allow the existence of a reflected wave, because of the impedance mismatch. Time independence leads not only to specific ratios between reflected, refracted, and incident waves, but also to conservation of frequency, which is proportional to the photon energy ($E = \hbar\omega$). This suggests that in its general implementation ($v_{interf} \neq 0$), the energy will not be constant. A device based on the effect described in Fig. 1 could be used to exchange energy in a controlled way with an optical wave. Techniques for continuous and efficient conversion of the photon energy — or, equivalently, of wavelength — are very interesting for optical communications. Most of the nowadays available techniques rely on inelastic optical processes. For example, stimulated Raman scattering has been successfully employed for frequency conversion and lasing [36–38]. Unfortunately inelastic processes usually require high intensities, and the frequency can hardly be tuned continuously on wide ranges. Finding new approaches to such a task is a challenging problem. Recently, Reed *et al.* [39] have proposed a way to change the color of light by capturing it on a propagating shock wave front and successive reemission. Dynamic reflection with plasma mirrors has also been suggested towards the development of laser-driven attosecond sources for use in fields from materials science to molecular biology [40].

Actually, in its most general form, the requirement for the electromagnetic energy of a wave traveling in a medium to be *not* constant in time is that the medium response has an explicit time dependance in its dielectric permittivity or in its magnetic permeability. The conceptually simplest energy-shifting device would be, therefore, a single, homogeneous dielectric medium, with a time dependent ϵ . The physical mechanism of such device could be referred to as a “time refraction” [41–57]. The light wave, indeed, gets refracted, by a continuous variation of the refractive index, similarly to what happens in a mirage. In a mirage, however, the refraction is due to a change of the refractive index *in space*, with the effect of elastically steering the wavevector \mathbf{k} . Here, on the other hand, the refractive index changes *in time* domain. Thus, the shifted quantity is the frequency ω rather than the wave vector \mathbf{k} . Since there is only a single time dimension, the possible shift can be only in the magnitude of ω , with no equivalent of the beam steering, which requires a multidimensional space.

I suggest therefore to consider two kind of “energy lifters”, the one based on refraction and reflection (where shifts are due to Doppler effect), and the one based on the spatially homogeneous time-refraction. An important detail is that it is harder to achieve an “abrupt interface” over time than over space domain. The abrupt interface in space is an ubiquitous building block

in optical systems. The practical difficulty for sharp interfaces in time derives from the required fast switching of ϵ on the scale of a period of the electromagnetic oscillation (femtoseconds, at optical wavelengths) [47]. In space interfaces, the requirement is abruptness over the wavelength scale (micron), a more accessible task for present-day technologies.

All the effects suggested in this paper will benefit from nanophotonics in a twofold way. On one hand, spatial structuring at the wavelength scale is a powerful tool to control the properties of light propagation. I discuss an example of such structuring in Sec. 2.2. On the other hand, novel techniques (plasmonics, metamaterials) are emerging, which can be used to introduce strong and fast optical nonlinearities, and as such could be enabling ideas for the phenomena described in the present paper [58–60].

1.1 Doppler effect

In the following, I consider the case where both the light propagation and the interface motion are in the direction normal to the interface. In Fig. 2, the frame O' — the *frame of the interface*

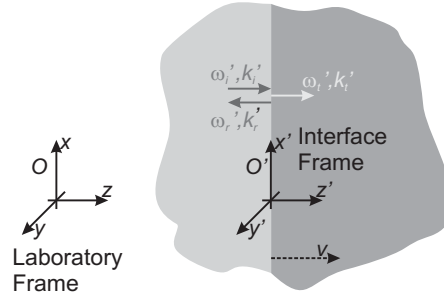


Fig. 2. Frames of reference

— is at rest with respect to the interface. I set the x' and y' axis of O' to lay in the plane of the interface, and the z' axis to be perpendicular to the interface. The media are moving with velocity $\mathbf{v} = v\mathbf{u}_z$, with $v > 0$, with respect to the reference frame O , the *frame of laboratory*. I first consider the case of two media with different permittivities (ϵ'_1, μ'_1 , and ϵ'_2, μ'_2) separated by a flat interface, which I refer to as the *material interface case*. The apex emphasizes that they are defined in the frame O' . The medium impedance is defined as [62]

$$\eta'_i = \sqrt{\frac{\mu'_i}{\epsilon'_i}}. \quad (1)$$

Throughout this work, I assume that ϵ'_1, μ'_1 , and ϵ'_2, μ'_2 are not frequency dependent. This means that *phase* and *group* velocity of light coincide. I consider also the case where the interface travels with respect to the media, and refer to it as the *traveling interface case*. Although this latter case might appear somewhat abstract, it is interesting for modeling reflection and refraction in devices like the *traveling wave refractor* suggested in Fig. 3, where the permittivities are modified by a time-dependent electro-optical effect.

1.1.1 Material Interface Case

For the observer O' , the case under study is just the classical case of reflection and refraction by the interface between two media at rest. The phase matching condition at any point of the still interface requires that a single plane wave generates a single reflected and a single refracted

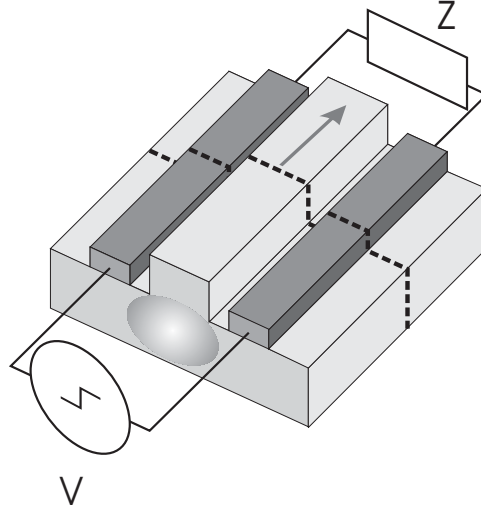


Fig. 3. Schematic representation of a *traveling wave refractor*. Light travels in a waveguide, whose core exhibits some electro-optic effect. The electro-optic effect is controlled by two side electrodes, which are terminated at the end side by a suitable impedance Z . For example, if Z matches the characteristic impedance of the electrode line, the traveling signal exhibits no reflection at Z . The driving signal is provided by a microwave generator V connected between the other sides of the electrodes, which inject a driving signal for the electro-optic effect. The wavefront of the microwave (dashed line) represents a moving interface between two portions of the medium, each with different refractive index. Hence, it can be viewed as an interface in relative motion with respect to two effective media. In order to focus on the effect of motion only, I make the simplifying assumption that the refractive index is everywhere constant in the core, except at the microwave interface, where it exhibits a discontinuity. This assumption is not realistic (it would require an infinite bandwidth in the frequency response of the nonlinearity of the refractive index): the device should be looked at only as a thought framework to discuss the effect of Doppler shift on refraction and reflection.

plane wave, and that frequency is conserved [61,63,64]. I label the frequency of any wave as ω' ($\omega' = \omega'_i = \omega'_r = \omega'_t$). The following relationships hold for the k-vectors and phase velocities:

$$\begin{aligned} k'_i &= \frac{\omega'}{c} n'_1; & k'_r &= -\frac{\omega'}{c} n'_1; & k'_t &= \frac{\omega'}{c} n'_2. \\ v'_{ph,i} &= \frac{c}{n'_1}; & v'_{ph,r} &= -\frac{c}{n'_1}; & v'_{ph,t} &= \frac{c}{n'_2}, \end{aligned} \quad (2)$$

where the subscripts i, r, t refer, respectively, to incident, reflected and refracted plane wave, and I have introduced the refractive indices

$$n'_i = \sqrt{\frac{\epsilon'_i \mu'_i}{\epsilon_0 \mu_0}}. \quad (3)$$

The time-averaged Poynting vectors $\mathbf{S}' = \mathbf{E}' \times \mathbf{H}'$ in O' are

$$\begin{aligned} \mathbf{S}'_i &= +\frac{E_i'^2}{\eta'_1} \mathbf{u}'_z; & \mathbf{S}'_r &= -\frac{\rho'^2 E_i'^2}{\eta'_1} \mathbf{u}'_z; & \mathbf{S}'_t &= +\frac{\tau'^2 E_i'^2}{\eta'_2} \mathbf{u}'_z; \\ S'_i &= \frac{E_i'^2}{\eta'_1}; & S'_r &= -\frac{\rho'^2 E_i'^2}{\eta'_1}; & S'_t &= \frac{\tau'^2 E_i'^2}{\eta'_2}, \end{aligned} \quad (4)$$

where I have introduced the symbols ϱ' and τ'

$$\varrho' = \frac{E'_r}{E'_i} = \frac{(\eta'_2 - \eta'_1)}{(\eta'_2 + \eta'_1)}; \quad \tau' = \frac{E'_t}{E'_i} = \frac{2\eta'_2}{(\eta'_2 + \eta'_1)}, \quad (5)$$

which are, respectively, the reflection and refraction coefficients of the electric fields in the frame O' . They are obtained by applying the boundary condition (equal tangential components in media 1 and 2) to the electric field \mathbf{E}' and to the magnetic field \mathbf{H}' .

The electromagnetic energy density $w' = 1/2(\mathbf{E}' \cdot \mathbf{D}' + \mathbf{B}' \cdot \mathbf{H}')$ in O' is [61], for each wave,

$$w'_i = \frac{E_i'^2}{c\eta'_1}; \quad w'_r = \frac{\varrho'^2 E_i'^2}{c\eta'_1}; \quad w'_t = \frac{\tau'^2 E_i'^2}{c\eta'_2}. \quad (6)$$

The conservation of energy can be expressed as

$$S'_i + S'_r - S'_t = 0, \quad (7)$$

as obtained by substituting Eqs. (5) into Eqs. (4). In Eq. (7), S'_i and S'_r are added with positive sign because the z' axis points from medium 1 towards the interface, whereas S'_t is added with negative sign because the z' axis points from interface towards medium 2. Since the Poynting vector and the electromagnetic energy are related as $\mathbf{S}' = w'\mathbf{v}'_{ph}$, the Eq. (7) can also be put in the form

$$w'_i v'_{ph,i} + w'_r v'_{ph,r} - w'_t v'_{ph,t} = 0. \quad (8)$$

For the photon fluxes, I follow the definition

$$N'_i = \frac{S'_i}{\hbar\omega'_i}; \quad N'_r = \frac{S'_r}{\hbar\omega'_r}; \quad N'_t = \frac{S'_t}{\hbar\omega'_t}, \quad (9)$$

which has a clear meaning in the context of the quantization of the field.

As there is no change in frequency upon reflection and refraction, from Eq. (7) one also trivially derives the conservation of the number of photons (Fig. 4)

$$N'_i + N'_r - N'_t = 0. \quad (10)$$

The phase matching condition must be satisfied at the interface also in O because the phases are Lorentz invariant. Hence, there is only a single reflected and a single refracted wave also for the moving interface. To calculate the frequencies ω_i , ω_r and ω_t and the k-vectors k_i , k_r and k_t , as they are measured by the O observer, I have to transform the 4-vectors which contain the information about ω' and k' of the three waves from the O' to the O reference frame, according to the Lorentz transformation. I obtain the expressions for the O observer as

$$\begin{aligned} \omega_i &= \gamma\omega'(1 + \beta n'_1); & \omega_r &= \gamma\omega'(1 - \beta n'_1); & \omega_t &= \gamma\omega'(1 + \beta n'_2); \\ k_i &= \gamma\frac{\omega'}{c}(n'_1 + \beta); & k_r &= -\gamma\frac{\omega'}{c}(n'_1 - \beta); & k_t &= \gamma\frac{\omega'}{c}(n'_2 + \beta), \end{aligned} \quad (11)$$

where I have followed the usual definitions $\beta = v/c$ and $\gamma = 1/\sqrt{1 - \beta^2}$. The Doppler shift of the frequency of the reflected and refracted wave is then expressed as

$$\omega_r = \omega_i \frac{1 - \beta n'_1}{1 + \beta n'_1}; \quad \omega_t = \omega_i \frac{1 + \beta n'_2}{1 + \beta n'_1}. \quad (12)$$

It is useful to find also the phase velocities of the incident, reflected and refracted waves for the O observer. From the general definition $v_{ph} = \omega/k$ it is

$$v_{ph,i} = \frac{\omega_i}{k_i} = c \frac{1 + \beta n'_1}{n'_1 + \beta}; \quad v_{ph,r} = \frac{\omega_r}{k_r} = -c \frac{1 - \beta n'_1}{n'_1 - \beta}; \quad v_{ph,t} = \frac{\omega_t}{k_t} = c \frac{1 + \beta n'_2}{n'_2 + \beta}. \quad (13)$$

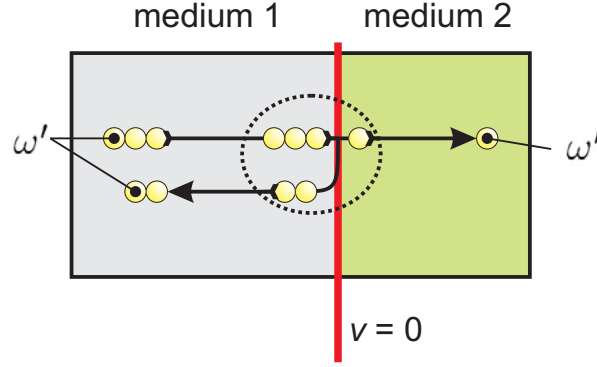


Fig. 4. Schematic representation of photon balance in the frame of reference at rest with media. Individual photons are pictorially represented as spheres. If I indicate with N'_i , N'_r and N'_t the instantaneous fluxes of incoming, reflected and refracted photons at the interface, I get, for the case in this figure, the ratio $\varrho'^2 = N'_r/N'_i = 2/3$ and $\tau'^2\eta'_1/\eta'_2 = N'_t/N'_i = 1/3$, where ϱ'^2 and $\tau'^2\eta'_1/\eta'_2$ are the classical power reflection and transmission coefficients. Indeed, the photon balance is equivalent to the classical power balance because of the uniformity of ω' .

The phase velocity is modified by a factor which can be regarded as an effective index due to the motion of the medium. The effective indices found here are in agreement with the calculations for normal incidence of existing literature [24, 65].

I now consider the transformation of the fields. At normal incidence, polarizations of wave are degenerate. If assume that in O' \mathbf{E}' is directed as \mathbf{u}'_x , then Maxwell equations imply that \mathbf{B}' is directed as \mathbf{u}'_y , and that \mathbf{D}' and \mathbf{H}' are also respectively directed as \mathbf{u}'_x and \mathbf{u}'_y . The Lorentz transformations in the particular case of translational velocity along z maintain the same directions, respectively, also for \mathbf{E} , \mathbf{B} , \mathbf{D} and \mathbf{H} . The transformed field components in O are

$$\begin{aligned}
 E_i &= \gamma E'_i(1 + \beta n'_1); & E_r &= \gamma \varrho' E'_i(1 - \beta n'_1); & E_t &= \gamma \tau' E'_i(1 + \beta n'_2); \\
 B_i &= \frac{\gamma E'_i}{c}(\beta + n'_1); & B_r &= \frac{\gamma \varrho' E'_i}{c}(\beta - n'_1); & B_t &= \frac{\gamma \tau' E'_i}{c}(\beta + n'_2); \\
 D_i &= \frac{\gamma E'_i}{c\eta'_1}(n'_1 + \beta); & D_r &= \frac{\gamma \varrho' E'_i}{c\eta'_1}(n'_1 - \beta); & D_t &= \frac{\gamma \tau' E'_i}{c\eta'_2}(n'_2 + \beta); \\
 H_i &= \frac{\gamma E'_i}{\eta'_1}(n'_1\beta + 1); & H_r &= \frac{\gamma \varrho' E'_i}{\eta'_1}(n'_1\beta - 1); & H_t &= \frac{\gamma \tau' E'_i}{\eta'_2}(n'_2\beta + 1),
 \end{aligned} \tag{14}$$

where E'_i is the electric field in the reference frame O' . The results found here are consistent with existing literature [26].

From Eqs. (14), two general results should be pointed out. First, the ratio $E'/H' = \eta' = E/H = \eta$ for any plane wave does not depend on the state of motion of the dielectric. This is not trivially expected from Lorentz transformation: for example, the ratio E/B does depend on the state of motion. I emphasize, however, that E/H is non invariant for a general Lorentz transformation. A sufficient condition for the invariance of η is that the transformation is parallel to the wave vector and the wave is purely transversal. Second, since $-1 < \beta < 1$, the two fields B and D never change sign, but the fields E and H do: this happens for waves traveling in the opposite direction to the translation of the medium, in the critical condition ($|\beta| > n_i'^{-1}$).

The time-averaged Poynting vectors $\mathbf{S} = \mathbf{E} \times \mathbf{H}$ in O are

$$\begin{aligned}\mathbf{S}_i &= +\frac{\gamma^2 E_i'^2}{\eta_1'}(1 + \beta n_1')^2 \mathbf{u}_z; & \mathbf{S}_r &= -\frac{\gamma^2 \varrho'^2 E_i'^2}{\eta_1'}(1 - \beta n_1')^2 \mathbf{u}_z; \\ \mathbf{S}_t &= +\frac{\gamma^2 \tau'^2 E_i'^2}{\eta_2'}(1 + \beta n_2')^2 \mathbf{u}_z.\end{aligned}\tag{15}$$

The sign of the Poynting vector is invariant for any value of β because the change of sign in the critical condition $|\beta| > n_1'^{-1}$ occurs simultaneously for \mathbf{E} and \mathbf{H} .

The electromagnetic energy density $w = 1/2(\mathbf{E} \cdot \mathbf{D} + \mathbf{B} \cdot \mathbf{H})$ in O is

$$\begin{aligned}w_i &= \frac{\gamma^2 E_i'^2}{c\eta_1'}(1 + \beta n_1')(n_1' + \beta); & w_r &= \frac{\gamma^2 \varrho'^2 E_i'^2}{c\eta_1'}(1 - \beta n_1')(n_1' - \beta); \\ w_t &= \frac{\gamma^2 \tau'^2 E_i'^2}{c\eta_2'}(1 + \beta n_2')(n_2' + \beta),\end{aligned}\tag{16}$$

where I note that in critical condition $|\beta| > n_1'^{-1}$ the energy density becomes negative, but the relationship $\mathbf{S} = w\mathbf{v}_{ph}$ still holds, as for media at rest.

To prove the conservation of energy, one must take into account the mechanical energy which is transferred to the material system by the electromagnetic pressure applied by the waves to the interface. The momentum density (momentum per unit volume) \mathbf{g} carried by the plane wave is [61]

$$\mathbf{g} = \mathbf{D} \times \mathbf{B} = \frac{\mathbf{S}}{v_{ph}^2},\tag{17}$$

where the last equality is a consequence of the relationships $\mathbf{D} = \mathbf{E}/\eta v_{ph}$ and $\mathbf{B} = \mathbf{H}\eta/v_{ph}$, which hold for any state of inertial motion, as directly derived from Eqs. (14). The energy per unit time per unit area ΔE exchanged between the wave and the interface is the momentum flux ($\mathbf{g}v_{ph}$) diminished by the momentum per unit time per unit area stored in the space created by the interface motion ($\mathbf{g}v$). Since \mathbf{g} and \mathbf{S} are related by Eq. (17), one can show that the mechanical energy flux is equal to the excess energy per unit time per unit area ΔE injected to the interface by the electromagnetic waves, which is the balance of Poynting vectors of the waves, diminished by the energy per unit time per unit area stored in the space created by the interface motion:

$$\begin{aligned}\Delta E &= w_i(v_{ph,i} - \beta c) + w_r(v_{ph,r} - \beta c) - w_t(v_{ph,t} - \beta c) \\ &= \frac{E_i'^2}{\eta_1'}(1 + \beta n_1') - \frac{\varrho'^2 E_i'^2}{\eta_1'}(1 - \beta n_1') - \frac{\tau'^2 E_i'^2}{\eta_2'}(1 + \beta n_2') \neq 0.\end{aligned}\tag{18}$$

The last line of Eq. (18), when compared to Eqs. (15) and (11), suggests to repeat the calculation for the photon flux instead of the energy flux. I divide the terms of Eq. (18) by $\hbar\omega$, where ω is the respective frequency of each term, as calculated by Eqs. (11). Thus, I calculate the photon balance as the difference ΔN between the incoming and outgoing photon fluxes of the waves, diminished by the stored photons in the space created by the interface motion.

$$\begin{aligned}\Delta N &= \frac{w_i}{\hbar\omega_i}(v_{ph,i} - \beta c) + \frac{w_r}{\hbar\omega_r}(v_{ph,r} - \beta c) - \frac{w_t}{\hbar\omega_t}(v_{ph,t} - \beta c) \\ &= \frac{E_i'^2}{\gamma\hbar\omega'\eta_1'} \frac{(1 + \beta n_1')}{(1 + \beta n_1')} - \frac{\varrho'^2 E_i'^2}{\gamma\hbar\omega'\eta_1'} \frac{(1 - \beta n_1')}{(1 - \beta n_1')} - \frac{\tau'^2 E_i'^2}{\gamma\hbar\omega'\eta_2'} \frac{(1 + \beta n_2')}{(1 + \beta n_2')} \\ &= \frac{E_i'^2}{\gamma\hbar\omega'} \left(\frac{1}{\eta_1'} - \frac{\varrho'^2}{\eta_1'} - \frac{\tau'^2}{\eta_2'} \right) = 0,\end{aligned}\tag{19}$$

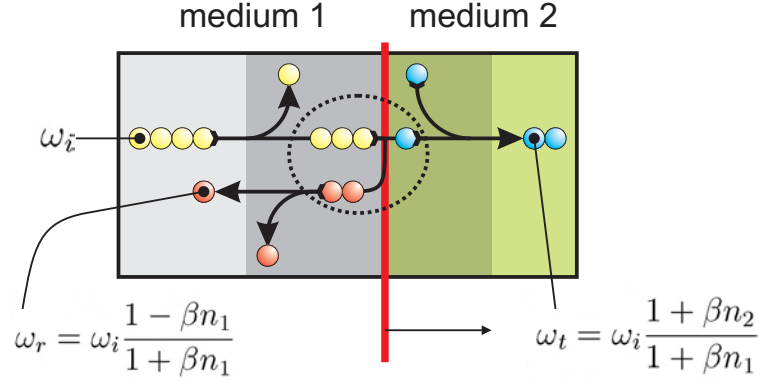


Fig. 5. Schematic representation of photon balance in a frame of reference O in motion with respect to the frame O' of media (axis conventions are given in Fig. 2). The interface moves with velocity $v\mathbf{u}_z$ in O as indicated by the arrow. Individual photons are pictorially represented as spheres. The ratios of instantaneous fluxes of photons — reflected versus incoming and refracted versus incoming — *at the interface* (i.e., inside the dashed circle) are *invariant* with respect to the status of motion (assumed inertial), and are equal to the power reflection and transmission coefficients ϱ'^2 and $\tau'^2\eta'_1/\eta'_2$ as calculated in the frame at rest with the interface. In this example, $\varrho'^2 = 2/3$ and $\tau'^2\eta'_1/\eta'_2 = 1/3$. The interpretation of this interesting result is that the interface between the two dielectrics acts as a number-conserving and invariant photon converter, regardless of its state of (inertial) motion. This joint invariance and conservation law is fully contained inside classical electrodynamics.

where ΔN vanishes because of Eq. (7). The interpretation of this last interesting result is that the interface between the two dielectrics acts as an number-conserving and invariant photon converter, regardless of its state of (inertial) motion, in quantitative consistency with both Doppler shifts and the conservation of energy. This joint invariance and conservation law is fully contained inside classical electrodynamics. The interpretation is schematically shown in Fig. 5.

The effects of motion of the medium are summarized in Table 1, which reports the effective index (labeled as n with no apex) due to motion, calculated from Eqs. (13), and the invariance of the impedance η' , as observed in Eqs. (14). Such invariance, however, is true only for transversal waves propagating parallel to the motion of the medium [66].

1.1.2 Traveling Interface Case

In order to provide a model for the traveling wave reflector, I assume that the media are at rest *in the frame O* . Thus, *only the interface* is at rest in the frame O' . Since the media are now in motion with z -velocity $-v$ with respect to O' , the calculation of frequency and k -vectors can be carried on as in the previous paragraphs, provided that I use the effective refractive index ($n = c/v_{ph}$) calculated from Eqs. (13) and reported in Table 1, instead of the index of the medium at rest.

The frequency is still conserved in frame O' because the phase matching condition still applies (it depends on the motion condition of the interface only, which is at rest). Thus, it is again $\omega'_i = \omega'_r = \omega'_t = \omega'$ as in Sec. (1.1.1). All the equations of Sec. (1.1.1) that depend on

Stationary Dielectric	Moving Dielectric
$n' = \sqrt{\frac{\epsilon'\mu'}{\epsilon_0\mu_0}}; \quad \eta' = \sqrt{\frac{\mu'}{\epsilon'}}$	$n = \frac{n' \pm \beta}{1 \pm n'\beta}; \quad \eta = \eta';$
$\mathbf{E}'; \quad \mathbf{B}' = \frac{ \mathbf{E}' }{c/n'};$	$\mathbf{E} = \gamma\mathbf{E}'(1 \pm \beta n'); \quad \mathbf{B} = \frac{ \mathbf{E} }{c/n};$
$\mathbf{D}' = \epsilon'\mathbf{E}'; \quad \mathbf{H}' = \frac{\mathbf{B}'}{\mu'}; \mathbf{H}' = \frac{ \mathbf{E}' }{\eta'}$	$\mathbf{D} = \epsilon'\mathbf{E} \frac{n}{n'}; \quad \mathbf{H} = \frac{\mathbf{B}}{\mu} \frac{n'}{n}; \mathbf{H} = \frac{ \mathbf{E} }{\eta}$

Table 1. Effect of motion of medium on the relationships between fields \mathbf{E} and \mathbf{B} , \mathbf{D} and \mathbf{H} of electromagnetic waves, assumed transversal, and propagating inside a dielectric medium, assumed isotropic when at rest. The waves are assumed to propagate along the direction of motion of the dielectric. β is the ratio of the speed of the dielectric and the speed of light in vacuum. The + (-) sign applies to waves co-propagating (counter-propagating) with respect to the motion of the dielectric. The permittivity and permeability of the immobile dielectric are, respectively, ϵ' and μ' . The refractive indices of immobile and moving dielectric are, respectively n' and n , where the latter can be defined as the ratio of the velocity of light in vacuum and the phase velocity of light in the moving dielectric (hence, it depends on the wave being co- or counter-propagating with respect to the dielectric).

the index of refraction must be now modified. Equations (2) must be replaced by

$$\begin{aligned}
k'_i &= \frac{\omega'}{c} \frac{n_1 - \beta}{1 - \beta n_1}; & k'_r &= -\frac{\omega'}{c} \frac{n_1 + \beta}{1 + \beta n_1}; & k'_t &= \frac{\omega'}{c} \frac{n_2 - \beta}{1 - \beta n_2}. \\
v'_{ph,i} &= c \frac{1 - \beta n_1}{n_1 - \beta}; & v'_{ph,r} &= -c \frac{1 + \beta n_1}{n_1 + \beta}; & v'_{ph,t} &= c \frac{1 - \beta n_2}{n_2 - \beta}.
\end{aligned} \tag{20}$$

The expressions of the reflection and refraction coefficients in Eqs. (5) are questionable in the rest frame of a traveling interface. In fact, Eqs. (5) are derived from the two following boundary conditions: a) the ratio of the magnitude of the total electric field over the magnitude of the total magnetic field is the impedance η'_1 in medium 1 and η'_2 in medium 2, and b) energy is conserved at the interface, leading to

$$\text{a) } \eta'_1 \frac{1 + \varrho'}{1 - \varrho'} = \eta'_2; \quad \text{b) } \frac{1}{\eta'_1} - \frac{\varrho'^2}{\eta'_1} = \frac{\tau'^2}{\eta'_2}. \tag{21}$$

With this approach, continuity of the tangential components of the electric field \mathbf{E}' and to the magnetic field \mathbf{H}' derives from the conservation of energy, and is not inferred from Maxwell equations. In my opinion, the derivation from conservation of energy is a sounder procedure. In principle, time-dependent Maxwell equations do not require these tangential components to be continuous. For example, $\nabla \times \mathbf{E} = -\partial\mathbf{B}/\partial t$, does not guarantee that \mathbf{E} is continuous (rather, that the vector $\mathbf{E} + \partial\mathbf{A}/\partial t$ is, where \mathbf{A} is the vector potential) [64]. Thus, one can question the continuity of \mathbf{E} at the interface if the electromagnetic energy is not conserved. The relaxation of continuity requirement allows for alternate conditions instead of the one shown in Eq. (21b). I will briefly outline a possible alternate approach in next section.

If conservation of energy of Eq. (21b) is assumed, then Eqs. (5) are valid also for this case, on the ground that the impedance η' is invariant (Table 1). I also assume that the bandwidth of the response of \mathbf{D} and \mathbf{H} to \mathbf{E} and \mathbf{B} is infinite. While this is certainly not valid, I aim at providing here a simplified picture to highlight a few basic differences between this case and the material interface of Sec. 1.1.1. The assumption of infinite bandwidth definitely deserves strong criticism. In any case, the following calculations should be considered only as indications for future discussions [47].

The expressions of the time-averaged Poynting vectors in Eqs. (4) are left unchanged because η is invariant. This only means that it is possible to express the amplitude of Poynting vector of a plane wave as E^2/η independently on the state of motion: the magnitude itself is not invariant and depends on the state of motion as calculated in Eqs. (14).

The electromagnetic energy density $w' = 1/2(\mathbf{E}' \cdot \mathbf{D}' + \mathbf{B}' \cdot \mathbf{H}')$ in O' is, for each wave,

$$w'_i = \frac{E_i'^2}{c\eta'_1} \frac{1 - \beta n_1}{n_1 - \beta}; \quad w'_r = \frac{E_r'^2}{c\eta'_1} \frac{1 + \beta n_1}{n_1 + \beta}; \quad w'_t = \frac{E_t'^2}{c\eta'_2} \frac{1 - \beta n_2}{n_2 - \beta}. \quad (22)$$

The conservation of energy can be expressed as in Eqs. (7) and (8) and the conservation of photon flux also holds, as in Eq. (10).

The expressions of frequency and k-vectors for the O observer are

$$\begin{aligned} \omega_i &= \gamma \omega' (1 + \beta \frac{n_1 - \beta}{1 - \beta n_1}) = \gamma \omega' (\frac{1 - \beta^2}{1 - \beta n_1}) = \frac{\omega'}{\gamma} (\frac{1}{1 - \beta n_1}); \\ \omega_r &= \frac{\omega'}{\gamma} (\frac{1}{1 + \beta n_1}); \quad \omega_t = \frac{\omega'}{\gamma} (\frac{1}{1 - \beta n_2}); \\ k_i &= \gamma \frac{\omega'}{c} (\frac{n_1 - \beta}{1 - \beta n_1} + \beta) = \gamma \frac{\omega' n_1}{c} (\frac{1 - \beta^2}{1 - \beta n_1}) = \frac{\omega' n_1}{\gamma c} (\frac{1}{1 - \beta n_1}); \\ k_r &= -\frac{\omega' n_1}{\gamma c} (\frac{1}{1 + \beta n_1}); \quad k_t = \frac{\omega' n_2}{\gamma c} (\frac{1}{1 - \beta n_2}). \end{aligned} \quad (23)$$

If I now calculate the phase velocity ($v_{ph} = \omega/k$), I find

$$v_{ph,i} = \frac{\omega_i}{k_i} = \frac{c}{n_1}; \quad v_{ph,r} = \frac{\omega_r}{k_r} = -\frac{c}{n_1}; \quad v_{ph,t} = \frac{\omega_t}{k_t} = \frac{c}{n_2}, \quad (24)$$

consistently with the fact that the media are still for the observer O .

The Doppler shift of the frequency of the reflected and refracted wave is then expressed as

$$\omega_r = \omega_i \frac{1 - \beta n_1}{1 + \beta n_1}; \quad \omega_t = \omega_i \frac{1 - \beta n_1}{1 - \beta n_2}, \quad (25)$$

where it is interesting to notice that the Doppler shift of reflected wave is unchanged with respect to Eq. (12), but the shift of the transmitted wave is different.

The transformed field components in O are

$$\begin{aligned}
E_i &= \frac{E'_i}{\gamma} \frac{1}{(1 - \beta n_1)}; & E_r &= \frac{\varrho' E'_i}{\gamma} \frac{1}{(1 + \beta n_1)}; & E_t &= \frac{\tau' E'_i}{\gamma} \frac{1}{(1 - \beta n_2)}; \\
B_i &= \frac{E'_i}{\gamma c} \frac{n_1}{(1 - \beta n_1)}; & B_r &= -\frac{\varrho' E'_i}{\gamma c} \frac{n_1}{(1 + \beta n_1)}; & B_t &= \frac{\tau' E'_i}{\gamma c} \frac{n_2}{(1 - \beta n_2)}; \\
D_i &= \frac{E'_i}{\gamma \eta'_1 c} \frac{n_1}{(1 - \beta n_1)}; & D_r &= \frac{\varrho' E'_i}{\gamma \eta'_1 c} \frac{n_1}{(1 + \beta n_1)}; & D_t &= \frac{\tau' E'_i}{\gamma \eta'_2 c} \frac{n_2}{(1 - \beta n_2)}; \\
H_i &= \frac{E'_i}{\gamma \eta'_1} \frac{1}{(1 - \beta n_1)}; & H_r &= -\frac{\varrho' E'_i}{\gamma \eta'_1} \frac{1}{(1 + \beta n_1)}; & H_t &= \frac{\tau' E'_i}{\gamma \eta'_2} \frac{1}{(1 - \beta n_2)};
\end{aligned} \tag{26}$$

where the symbols ϱ' and τ' are, as already said above, unchanged from Eqs. (5).

The time-averaged of Poynting vectors $\mathbf{S} = \mathbf{E} \times \mathbf{H}$ in O are

$$\begin{aligned}
\mathbf{S}_i &= +\frac{E_i'^2}{\gamma^2 \eta'_1} (1 - \beta n_1)^{-2} \mathbf{u}_z; & \mathbf{S}_r &= -\frac{\varrho'^2 E_i'^2}{\gamma^2 \eta'_1} (1 + \beta n_1)^{-2} \mathbf{u}_z; \\
\mathbf{S}_t &= +\frac{\tau'^2 E_i'^2}{\gamma^2 \eta'_2} (1 - \beta n_2)^{-2} \mathbf{u}_z.
\end{aligned} \tag{27}$$

The electromagnetic energy density $w = 1/2(\mathbf{E} \cdot \mathbf{D} + \mathbf{B} \cdot \mathbf{H})$ in O is

$$w_i = \frac{E_i'^2 n_1}{c \gamma^2 \eta'_1} (1 - \beta n_1)^{-2}; \quad w_r = \frac{\varrho'^2 E_i'^2 n_1}{c \gamma^2 \eta'_1} (1 + \beta n_1)^{-2}; \quad w_t = \frac{\tau'^2 E_i'^2 n_2}{c \gamma^2 \eta'_2} (1 - \beta n_2)^{-2}. \tag{28}$$

Even though I have limited the analysis to $\beta \leq n_1^{-1}$ and $\beta \leq n_2^{-1}$, I mention that the energy density as resulting from Eqs. (28) does not become negative under any condition, consistently with the fact that media are at rest in the observer frame.

If I now follow the same reasoning as in Sec. 1.1.1, I obtain, in place of Eq. (19),

$$\begin{aligned}
\Delta N &= \frac{w_i}{\hbar \omega_i} (v_{ph,i} - \beta c) + \frac{w_r}{\hbar \omega_r} (v_{ph,r} - \beta c) - \frac{w_t}{\hbar \omega_t} (v_{ph,t} - \beta c) \\
&= \frac{E_i'^2}{\gamma \hbar \omega' \eta'_1} \frac{(1 - \beta n_1)^2}{(1 - \beta n_1)^2} - \frac{\varrho'^2 E_i'^2}{\gamma \hbar \omega' \eta'_1} \frac{(1 + \beta n_1)^2}{(1 + \beta n_1)^2} - \frac{\tau'^2 E_i'^2}{\gamma \hbar \omega' \eta'_2} \frac{(1 - \beta n_2)^2}{(1 - \beta n_2)^2} \\
&= \frac{E_i'^2}{\gamma \hbar \omega'} \left(\frac{1}{\eta'_1} - \frac{\varrho'^2}{\eta'_1} - \frac{\tau'^2}{\eta'_2} \right) = 0,
\end{aligned} \tag{29}$$

where I have found again that $\Delta N = 0$, because of Eq. (7). Therefore, the joint invariance and conservation law illustrated in Fig. 5 is valid also for this case, where the Doppler shift is now expressed by Eqs. (25).

1.1.3 Traveling Interface Case: an alternate approach

As anticipated while discussing Eqs. (21), conservation of electromagnetic energy can be questioned in the frame at rest with the interface, if the medium is moving in that frame. The question arises because refraction is a consequence of a partial sharing of energy between radiation and medium, this sharing is different at the two sides of the interface, and motion of the medium can thus take in or away different amount of energy at these two sides. I remark that

any modification of the boundary conditions for the fields does not change the Doppler shifts expressed by Eqs. (25), which do not depend on the electromagnetic field amplitudes.

I will now modify the approach to investigate an alternate condition instead of the conservation of energy expressed in Eq. (21b). I hypothesize, as a possible assumption directly in the frame of the medium (O), that there is no mechanical energy exchange at the moving interface, despite its motion. This assumption is taken on the ground that the radiation pressure is applied to a physically static object in frame O . If atoms do not move, it might be sensible to assume that they are not absorbing/releasing mechanical power. The reader should look at my suggestions with critical eye, since they contrast with existing literature [34]. Generally speaking, when the dielectric response is time-dependent, one should assume that the displacement vector \mathbf{D} cannot change instantaneously. This latter assumption derives, on one side, from the finite bandwidth of the material response. \mathbf{D} describes how the material responds to an external stimulus (\mathbf{E} field), hence its dependence on \mathbf{E} results from a convolution integral, which smoothes out the high frequency variations of \mathbf{E} . Second, time continuity of \mathbf{D} is also consistent with Maxwell equations. In fact, a finite discontinuity of \mathbf{D} or \mathbf{B} fields in time would make $\nabla \times \mathbf{E}$ and $\nabla \times \mathbf{H}$ divergent. Additional discussion on time-continuity of \mathbf{D} and \mathbf{B} is available in the literature [30,32]. Thus, I am led to study the pure effect of time continuity of \mathbf{D} and \mathbf{B} [56,57]. I consider a single transversal electromagnetic wave (with field magnitudes E_{1f}, H_{1f}), traveling across a homogeneous dielectric medium (no interface *in space*), in which I suppose it is possible to suddenly switch the dielectric response from ϵ_1, μ_1 to ϵ_2, μ_2 . As a consequence of the sudden switch, the wave splits into a forward- (with field magnitudes E_{2f}, H_{2f}) and a backward-propagating wave (E_{2b}, H_{2b}). Time continuity of \mathbf{D} and \mathbf{B} leads to

$$\epsilon_1 E_{1f} = \epsilon_2 (E_{2f} + E_{2b}); \quad \frac{\mu_1}{\eta_1} E_{1f} = \frac{\mu_2}{\eta_2} (E_{2f} - E_{2b}). \quad (30)$$

Solving for E_{2f} and E_{2b} , one gets

$$E_{2f} = \frac{E_{1f}}{2} \left(\frac{\epsilon_1}{\epsilon_2} + \frac{\eta_2 \mu_1}{\eta_1 \mu_2} \right); \quad E_{2b} = \frac{E_{1f}}{2} \left(\frac{\epsilon_1}{\epsilon_2} - \frac{\eta_2 \mu_1}{\eta_1 \mu_2} \right). \quad (31)$$

If the energy of the waves is now calculated, one finds that the electromagnetic energy is changed after the switch. It is interesting also to underline that even the net forward power flow (the difference between the power of forward and backward propagating waves) is different from the original power:

$$\Delta S_{2f} = E_{2f} H_{2f} - E_{2b} H_{2b} = \frac{E_{1f}^2}{\eta_1} \frac{n_1^2}{n_2^2} \neq E_{1f} H_{1f} = \frac{E_{1f}^2}{\eta_1}, \quad (32)$$

but the momentum density is conserved, as derived from Eqs. (17) and (32):

$$\Delta g_{2f} = g_{2f} - g_{2b} = \Delta S_{2f} \frac{n_2^2}{c^2} = \frac{E_{1f}^2}{\eta_1} \frac{n_1^2}{c^2} = g_{1f}. \quad (33)$$

Hence, there is no net variation of momentum in the electromagnetic field associated to a pure time variation of the refractive index. The waves are not applying any force to medium, and any variation of energy of the waves would not be due to a mechanical action, but rather to a direct transfer from and to the material as in Eq. (32). Equations (32) can be interpreted as the consequence of an infinitely fast interface [32]. Thus, one might assume the total energy variation *in frame O* to be negligible, at least for $\beta \ll 1$, compared to the material interface case discussed in Eq. (18) of Sec. 1.1.1, for which the mechanical exchange can be significant. The assumption of exact conservation of electromagnetic energy is difficult to justify because of Eq. (32). I suggest that in any case this argument requires deeper discussion. Here I just

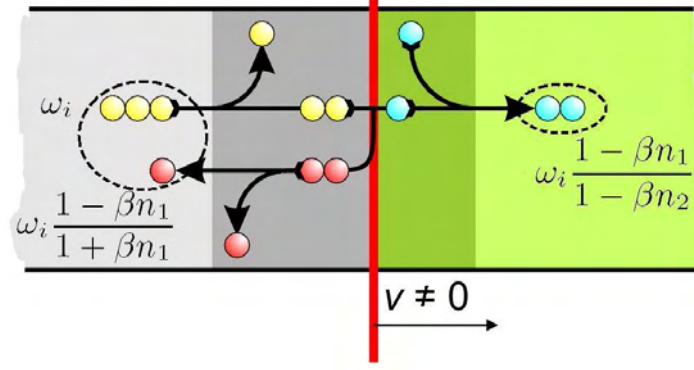


Fig. 6. Schematic representation of photon balance in the frame of reference O , in which the medium is at rest, and the interface moves with velocity $v\mathbf{u}_z$, as indicated by the arrow. Individual photons are pictorially represented as spheres. As opposed to what shown in Fig. 5, here the *overall* photonic fluxes (*not* the fluxes at the interface), are conserved and invariant. This conservation and invariance law is easier to access experimentally than the one in Fig. 5, because these are the fluxes which are actually measurable.

outline a possible alternate approach for the traveling interface case, remarking once again that the approach of Sec. 1.1.2, based on the conservation of electromagnetic energy in frame O' , can be also criticized.

So, I proceed assuming conservation of energy *in the O frame instead of in the O' frame*. This does not imply that the algebraic sum of time averaged Poynting vectors is zero, but, rather, that the incoming power flux $E_i^2[(1 - \varrho^2)\eta_1^{-1} - \tau^2\eta_2^{-1}]$ equals the net energy density multiplied by the interface speed, $E_i^2[(1 + \varrho^2)\epsilon_1 - \tau^2\epsilon_2]\beta c$, which accounts for the substitution of the waves (incident and reflected with refracted, or viceversa, according to the sign of the speed), in the region where the dielectric properties are changed.

Thus, the two new boundary conditions, directly in the frame O , would be

$$\text{a) } \eta_1 \frac{1 + \varrho}{1 - \varrho'} = \eta_2; \quad \text{b) } \frac{1}{\eta_1} - \frac{\varrho^2}{\eta_1} - \frac{\tau^2}{\eta_2} = [(1 + \varrho^2)\epsilon_1 - \tau^2\epsilon_2]\beta c. \quad (34)$$

Since $\epsilon c = n/\eta$, the condition in Eq. (34b) can be expressed also as

$$\frac{(1 - \beta n_1)}{\eta_1} - \frac{\varrho^2(1 + \beta n_1)}{\eta_1} - \frac{\tau^2(1 - \beta n_2)}{\eta_2} = 0, \quad (35)$$

which is equivalent to assume the Eq. (18) to be false for the traveling interface case. Insertion of Eqs. (23) in Eq. (35) leads to the conclusion that the condition of Eq. (34b) is equivalent to

$$\frac{1}{\eta_1(\hbar\omega_i)} - \frac{\varrho^2}{\eta_1(\hbar\omega_r)} - \frac{\tau^2}{\eta_2(\hbar\omega_t)} = 0, \quad (36)$$

i.e., to the conservation of photon fluxes shown in Fig. 6. Under the assumptions taken here, invariance of photon fluxes also holds (calculations are not shown). As repeatedly underlined, the conservation of energy in frame O can be questioned. Fortunately, however, the thereof deduced conservation law of photon flux is, in principle, directly accessible by experiment, indicating an interesting avenue for future experimental investigations. Would the assumption proposed here describe the phenomenon correctly, photon energy could be modified (by Doppler shift), without (or with no significant) variation of the total electromagnetic energy. In other words, the traveling interface would act, in this case, as an electromagnetic energy “rearranger” among photons.

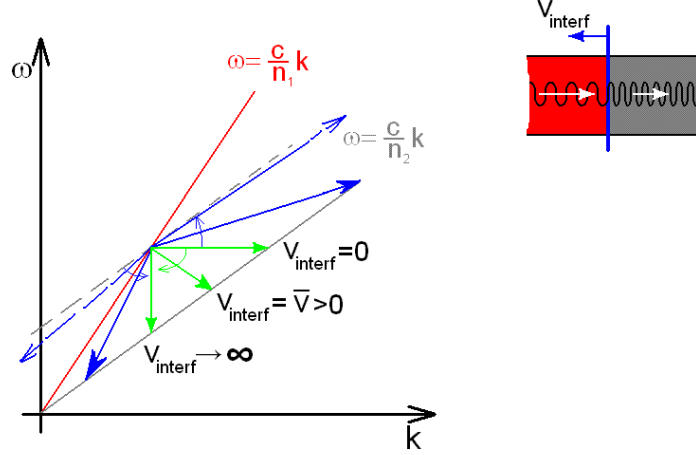


Fig. 7. The effect of an homogeneous lifting of the refractive index from the n_1 to the n_2 value can be looked at as the limiting case for $v_{interf} \rightarrow \infty$ of the speed of a counterpropagating (green arrows) interface. The case of a copropagating (blue arrows) interface is an intriguing one: at high speed — i.e., in the regime approaching the onset of the event horizons — critical phenomena are expected. This is a rich terrain for future investigations. The exact expressions for the transitions of ω and k can be obtained from Eqs. (23). The limiting case for $v_{interf} \rightarrow \infty$ is derived from Eq. (37).

1.2 Time-dependent refraction

It is a simple consequence of translational invariance that the wavevector k of an electromagnetic wave propagating in a homogeneous and non-absorbing dielectric with a time-dependent refractive index $n(t)$ is a conserved quantity [56,57]. As the frequency is related to the wavevector and the refractive index by $\omega = \frac{c}{n}k$, where c is the velocity of light in vacuum, a change of refractive index by δn results in a change of the frequency of a plane wave by

$$\frac{\delta\omega}{\omega} = -\frac{\delta n}{n_0 + \delta n} \simeq -\frac{\delta n}{n_0}. \quad (37)$$

The energy required for the frequency change is provided by the work done while changing the refractive index of the medium. I emphasize that to achieve energy lifting, the index change must be performed with the medium *loaded with optical energy*, otherwise one only modifies the material response.

This effect can be used in a photonic device to shift the carrier frequency of a wave-packet (light pulse), without dramatically affecting the pulse shape. In practice, one needs to trigger the refractive index shift once the pulse has entered the medium, in such a way that the shift completes before the pulse starts exiting. In other words, the traveling pulse must be fully contained in the medium during the whole index shift process. The optical linearity of the medium guarantees that the different k -components are decoupled, so that the pulse shape is preserved in both the real and the k -space.

It is instructive to picture the time-dependent refraction as the limiting case of a Doppler shift due to a counterpropagating interface for the speed of the interface tending to infinity. This is illustrated in Fig. 7. In the following, I limit my design goals to the lifting effect of the “time-dependent refraction” for simplicity. The exploitation of the Doppler shift in the high-speed copropagating interface regime is indicated as a rich terrain for future investigations.

2 SAMPLE DESIGNS FOR A PHOTON ENERGY LIFTER

Unfortunately, the experimental implementation of “time-dependent refraction” described in Sec. 1.2 is very demanding for available technology. As the travel time $\tau_{travel} = L/v_g$ of the pulse across the structure must be longer than the pulse duration τ_{pulse} plus the switching time τ_{sw} , the device length L has to be longer than $L_{min} = v_g(\tau_{pulse} + \tau_{sw})$. For realistic values of τ_{pulse} and τ_{sw} of the order of a few tens of picoseconds, and group velocities v_g of the order of a significant fraction of c , L_{min} can be as long as some millimeters. Such a length it is undesirable in the perspective of miniaturization and integration. It becomes apparent that one should increase the travel time across the structure. I am therefore led to investigate periodic photonic structures with particular dispersion relation, in which the magnitude of the group velocity is significantly reduced*.

Dynamical photonic structures, in which the optical constants of the medium can be modulated while the light is propagating inside it, have been recently introduced and are now attracting a great deal of interest from both the theoretical and experimental side (for a review, see e.g. [67]). Structures of this kind, originally suggested for stopping the light, open up an intriguing research area, in particular, for storing or manipulating optical information [68–70]. Here I face the photon energy conversion problem exploiting the simple idea of changing the refractive index of the structure, and thus the photon dispersion, while the pulse is propagating across the structure. This idea is illustrated on a realistic example inspired by presently available technology.

2.1 Single-cavity lifter

It is instructive to consider as first step a single, time-dependent optical microcavity. The frequency shift can be achieved with the following procedure: a) injection of electromagnetic energy in the cavity; b) shift of the resonance frequency, e.g. by a change of refractive index; c) release of the frequency-shifted electromagnetic energy. The microcavity is a fundamentally different solution with respect to the homogeneous medium, in that light is injected in a localized state. To quantitatively illustrate the lifter principle, I performed Finite Difference Time Domain (FDTD) simulations of a single $\lambda/2$ time-dependent cavity (Fig. 8).

In the microcavity approach, a fundamental trade-off in the trapping capability can be emphasized. On one side, one wants a high quality factor Q , to effectively achieve a long storage time once the cavity has been charged. This gives longer time to apply the frequency shift before the optical energy is released, thus adding practical flexibility to the device implementation. On the other side, a high quality factor means a very narrow bandwidth. This is undesirable for optical pulse processing, because the energy transfer between the incident charging wave and the cavity itself is limited to this frequency window. This results both in strong distortion of time-limited pulses, and in low efficiency in the cavity charging. The impact of the narrow bandwidth is evident from the example shown in Fig. 8. Almost independently on the spectral shape of the charging pulse (in this example, I use a Gaussian pulse lasting few tens ps), the energy exits as a slow, exponentially decaying wave, according to the characteristic Lorentzian filtering of the cavity. In Fig. 8, the output peak intensity is lower than input by almost 2 orders of magnitude. One should notice two additional undesirable features. First, the light exits also from the input side. This appears in Fig. 8 as a change of sign of Poynting vector at input side (dashed line) at time $\simeq 30$ ps. As implied by the symmetry of the structure, energy exits from both sides with the same amplitude (in the figure, this is partially hidden by the 30 times magnification). Second, a fraction of the stored energy unavoidably exits before the index shift (this feature is recognizable in the spectrum, as the solid bump at 1550.25 nm).

*Single optical microcavity can localize strongly the light and, in principle, are suitable for changing the photon energy. However, these structures strongly distort pulses.

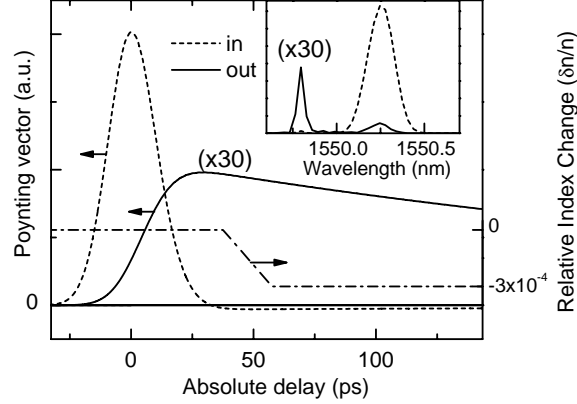


Fig. 8. Finite difference Time Domain (FDTD) simulation of the frequency shift in a sample time-dependent single Fabry-Perot microcavity (8.5 period Distributed Bragg Reflectors, with $\Delta n = 2$ index contrast). The dash (solid) line shows the amplitude of the Poynting vector at the input (output) side versus time. The inset shows the spectra of respective electric fields (the resolution of the spectrum of the output is limited by the time window of the simulation).

The comparison between the homogenous medium and the single cavity enlightens the path towards a solution which combines the respective advantages. A larger bandwidth than the one provided by the single microcavity is needed for the applications, but without sacrificing the light trapping ability of optical microcavities. I achieve this goal by resorting to coupled microcavities.

2.2 Coupled Resonator Optical Waveguide (CROW) lifter

Various photonic systems have been recently investigated to lower the group velocity of light. Line-defect photonic crystals [73] and coupled resonator optical waveguides (CROW) [74–76] are among the most promising ones.

Here I focus my attention on the case of a CROW structure, i.e. a spatially periodic many-cavity system, in which the degeneracy of the single cavity modes is lifted by the coupling between neighboring cavities through the inter-cavity mirrors. As a result, a miniband is created (Fig. 9), whose dispersion law in the weak coupling limit (for the general expression, see, e.g., [78]) has the form:

$$\omega_0(k) = [\bar{\omega} - J \cos(k\ell)]. \quad (38)$$

The miniband is centered at the single cavity frequency $\bar{\omega}$ and its width is proportional to the coupling strength J [77]. Here, ℓ is the CROW period and the quasi-wavevector k is defined modulo integer multiples of the reciprocal lattice vector $2\pi/\ell$. As a consequence of the strong light localization in the cavity modes (Fig. 9), the group velocity is orders of magnitude lower than the one associated to the average refractive index of the structure.

A spatially homogeneous dependence of the refractive index of the form $n(x) = n_0(x)(1 + \epsilon)$ results in a frequency shift of the miniband, i.e., $\omega_\epsilon(k) = \omega_0(k)/(1 + \epsilon)$. Provided the electromagnetic field dynamics is limited to the miniband states only (adiabatic regime) [79], a variation in time of the refractive index via $\epsilon(t)$ implies a coherent frequency shift of the whole wavepacket in the same way as discussed for the homogeneous case. The adiabatic requirement implies that the tuning time τ_{sw} be much larger than the inverse of the minimum frequency separation $1/\Delta\Omega$ between the miniband and the nearest allowed photonic states, shown schematically in Fig. 9. In semiconductors, the refractive index n can be modulated,

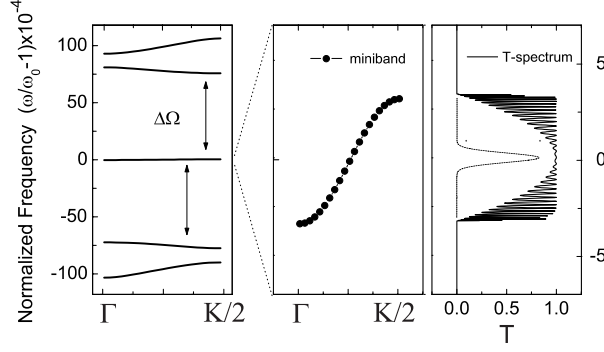


Fig. 9. Band structure of the 1D model of the CROW (left panel). The arrows indicate the frequency separation $\Delta\Omega$ between the miniband and the nearest allowed photonic states. Enlarged view of miniband (central panel). Transmission spectrum and spectral shape of the signal pulse, chosen to fit in the almost flat region of the spectrum (right panel). For the actual parameters see text.

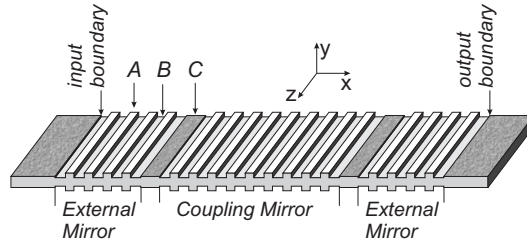


Fig. 10. Simplified schematic representation of the CROW structure. For simplicity, I have represented the external dielectric mirrors with only 4 periods instead of 13, and the inter-cavity – coupling – mirrors with only 9 periods instead of 27. Only 2 cavities instead of 45 have been shown. Light travels in the positive x direction.

e.g., by changing the free carrier density [80]. In particular, in Si, relative index modulation of the order of $\sim 10^{-4}$ has been recently demonstrated in the GHz range [81].

In a finite CROW system, for which the impedances are carefully matched at the input and output interfaces, the central part of the miniband corresponds to a frequency window in which the transmittivity is flat and almost unity (Fig. 9). Provided the incident pulse resides in this spectral region, it can penetrate into the photonic structure and then travel across it. Importantly, the pulse shape conservation is achieved by limiting the spectral content of the input pulse (dotted line, right panel, Fig. 9) to the frequency interval where the dispersion is linear (central panel). As the travel time τ_{travel} depends on the group velocity [82], a strong reduction of v_g with respect to c implies a much looser lower bound L_{min} on the system length L in order for the refractive index modulation to be performed while the pulse is contained in the structure.

2.3 CROW design and FDTD simulations

The designed structure is composed by 45 1D Fabry-Perot microcavities, coupled to each other through 27-period Distributed Bragg Reflectors (DBRs). The mirrors and the cavities are constituted by quarter- and half-wavelength layers, respectively, and are centered at $\lambda_0 = 1550$ nm. The input-output mirrors are suitably designed in order to have a good impedance matching between the finite-1D photonic structure and input/output channels. Assigning letters A and B

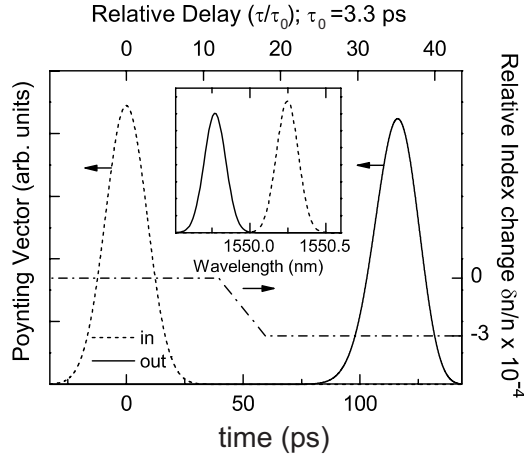


Fig. 11. FDTD simulation of the envelope of Poynting vectors at the input (dashed line, positive entering) and output boundary (solid line, positive exiting) of the coupled-cavities structure. Input and output boundaries are defined in Fig. 10. The refractive index of all the layers is time-dependent, as shown by the right y-axis. Upper time scale is relative to the delay (τ_0) in a homogeneous medium with the average refractive index of the 1D-structure. The inset shows the spectra of the input and output pulse electric fields.

to the mirror layers and C to each cavity layer, I choose their initial refractive indices equal to $n_A = 3$, $n_B = 2.426$ and $n_C = 2.688$, respectively. The choice of these specific values is related to the realistic implementation of this structure as a corrugated Si slab waveguide (see Fig. 10), whose realization is compatible with available Si technology. In quantitative detail, the guide includes a Si core layer of about 260 nm thickness, sandwiched between SiO_2 cladding layers. The index contrast between the two materials assures light confinement in the silicon core. The photonic structure (DBRs and cavities) is realized modulating the thickness of the Si slab, which leads to the effective refractive index values n_A , n_B and n_C for the fundamental transverse mode.

FDTD simulations have been performed on the 1D structure. The time dependence of the structure consists of a spatially homogeneous relative shift $\epsilon(t) = \delta n(x, t)/n_0(x)$ of the refractive index of each layer, triggered after the injection of the pulse and completed before the pulse exits. For simplicity, a linear time dependence of $\epsilon(t)$ has been considered. The number of cavities has been determined by the constrain that the pulse must be contained inside the structure during the time required for the index switch, assumed to be 20 ps. The final device length is about 370 μm . A slower switching time would simply imply a proportionally higher number of cavities and a correspondingly longer structure. Note that the minimum tuning time τ_{sw} for being adiabatic is, for these parameters, of the order of 10 fs, i.e. orders of magnitude shorter than the switching time of most existing materials. A shift $\delta n/n_0 = -3 \times 10^{-4}$ has been assumed, on the basis of realistically attainable values in semiconductor technology [83]. I mention that significantly larger index shifts, hence, frequency tuning, would be possible, just by resorting to electro-optic materials such as LiNbO_3 [83].

The results of the FDTD simulation of the pulse propagation are reported in Fig. 11. The pulse delay is 116 ps, i.e. a factor $\simeq 35$ larger than what expected in a homogeneous structure with the same length and same average refractive index. The resulting vacuum wavelength shift $2\pi c/\delta\omega = -\delta\lambda \simeq -0.49$ nm is shown in the inset, which corresponds to the expected $\delta\lambda/\lambda_0 \simeq |\delta n/n_0| = 3 \times 10^{-4}$. The distortion of the input pulse is negligible and the efficiency of conversion is larger than 95%.

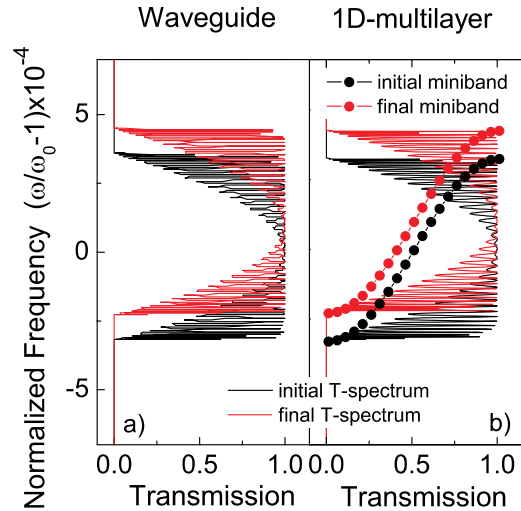


Fig. 12. (color online) A comparison between the calculated transmission spectra of the initial and shifted minibands in the case of a waveguide (a) and a 1D-multilayer structure (b). The miniband dispersion (full circles) in the 1D case is also plotted in (b).

Even though the FDTD simulation is performed on 1D time-dependent structure, the results are essentially applicable also to the quasi-1D slab waveguide structure of Fig. 10. This can be demonstrated by a full (time-independent) 2D simulation for the slab waveguide, performed using an eigenmode expansion method [84]. I assume a vertical symmetric (the y -direction) architecture, as sketched in Fig. 10. The physical parameters of the integrated device (length and thickness of the layers) have been chosen in order to maintain a good modal matching between input/output waveguides, cavities and DBRs. In this way the insertion losses in the resulting two dimensional CROW slab device appear to be negligible, of the order of 0.1 dB. In Fig. 12 the miniband spectra of the slab structure (panel a) and the 1D model of the CROW (panel b) are shown both at the initial time and after the spatially homogeneous relative shift of refractive index. The close similarity of the two graphs confirms that the 1D model and the corresponding 1D FDTD simulations provide an accurate description of light propagation through the slab waveguide system and of the predicted photonic lift effect.

2.4 Travelling wave design

Up to now the basic idea of the photon energy lifter was based on the hypothesis that the refractive index can be simultaneously changed in the whole structure while the pulse is travelling across it. Another possible scheme, which can simplify the experimental realization is what can be called a travelling-wave design [85]. In this scheme, the electrical field for the electro-optic effect is not applied simultaneously to the whole device, but is injected as a microwave from one end of the electrode pair. Electrodes work as a transmission line. In this design, the modulator speed is not limited by a lumped electrode capacitance but by the distributed impedance.

Since the photonic structure under study is designed for *optical* wavelengths, it behaves as a homogeneous medium at microwaves. Therefore, it is expected that the group velocity at microwaves is determined by the average refractive index, $n_{\mu w}$, of the structure and thus it is much higher than the group velocity of the optical pulse. Moreover, its wavelength being much shorter than the microwave rise time, the optical pulse sees an almost translationally invariant system with a time-dependent refractive index.

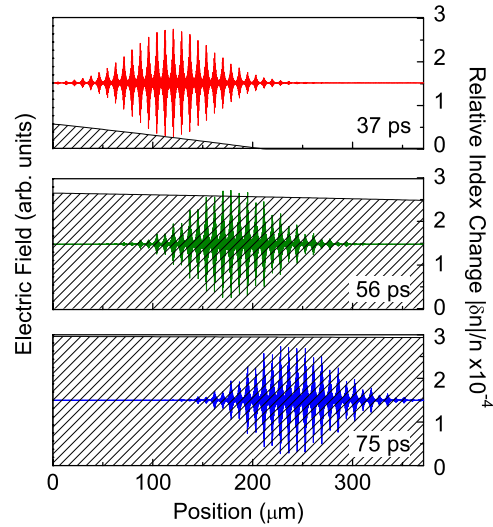


Fig. 13. (color online) Successive snapshots of the electric field of the optical wave and of the index-driving microwave at 37, 56 and 75 ps. The differently colored electric fields have an illustrative scope and refer to a blueshift of the input pulse wavelength. The structure of the pulse electric field reflects the coupled cavity structure (maxima are located in correspondence of C layers).

In order to verify that no spurious effect occur at the microwave front, I have performed 1D FDTD simulations for the coupled microwave and optical pulses. In the FDTD simulations, I assume a conservative value of $n_{\mu w}=3$ for the effective refractive index of the mixed Si/SiO₂ structure at microwaves: the optical group velocity v_g in my structure is therefore lower than the microwave group velocity $c/n_{\mu w}$ by over an order of magnitude. The microwave driver signal is taken as a smooth function $\propto [1 - \exp(-t/\tau)]$ with $\tau^{-1} = 100$ GHz. The microwave is sent into the structure with a 35 ps delay from the input light signal, i.e., when the injection of the light signal is essentially completed (Fig. 11). Sample electric field snapshots resulting from the combined optical and microwave simulations are reported in Fig. 13, where an instantaneous response of the refractive index to the microwave amplitude has been assumed. The results of the travelling-wave simulation are not distinguishable from the results of Fig. 11, which verifies the effectiveness of this second travelling wave scheme to shift the pulse carrier frequency.

2.5 Back to the single cavity design?

Designs of Sec. 2.2, 2.3 and 2.4 are quite satisfactory in terms of the expected performance but are too technologically demanding: it is quite unrealistic to rely on multicavity devices whose performance critically depends on the fact that cavities must match in size and where fabrication imprecisions of few nm risk to make the device useless. Ideally, one's desire is to avoid the need of multiple matching devices whenever possible. The question comes about whether I can go back to a single cavity device. Can I let a pulse into a single high-Q cavity, and at the same time limit the strong distortion seen in Fig. 8?

The answer is positive. The idea comes by considering that low distortion requires a large device bandwidth. Multimodal cavities, such as the ones used in mode locking, can have large bandwidth, and, simultaneously, high-Q factors. Spectrally wide pulses, injected in a single multimode cavity, coherently excite many modes. The requirement for low distortion are that the losses of the cavity are low and homogeneous across the cavity modes, the cavity is not dispersive, and unwanted nonlinearities are kept low.

There is, however, an additional intriguing possibility with multimode cavities. A coherently excited broadband pulse is localized in space inside the cavity, and travels within the confined space of the cavity with a period equal to the reciprocal of the cavity Free Spectral Range (FSR). If the total losses of the cavity are kept low, the pulse will make several round trips before decaying. Thus, I can repeatedly apply the index shift, as proposed in Sec. 1.2, in a selected region of the cavity while the pulse is passing there, and recover the initial starting value of the index when the pulse is outside such selected region. This allows the pulse to experience a refractive index shift which is monotonic in time, repeatedly recoiling when the pulse is away from the shifting region. This is possible even if the modulation of the index is driven by a stationary wave. The idea is illustrated in Fig. 14 in the case of a whispering gallery multimode cavity.

3 PRELIMINARY EXPERIMENTS

Pulsed functioning of optical whispering gallery resonators (WGRs) [71,86,87] is very interesting for many applications, such as Direct Frequency Comb Spectroscopy (DFCS) [88], optical comb generation and stabilization [89], optical clock distribution in integrated circuits [90], pulsed ringdown spectroscopy [91] and biosensing at single-molecule level [92–94]. Advantages of WGRs include compactness, mechanical stability and ultra-high demonstrated quality factors $Q > 10^{11}$ and finesse figures $\mathcal{F} > 10^7$ [95]. For steady-state pulsed functioning of the WGR, resonator's eigenmodes must be uniformly spaced in frequency, and excited by preserving phase-coherence, as in mode-locked lasers [96]. This constrain in WGRs appears to be within close reach, after the recent demonstration that the frequency spectrum of suitably fabricated WGRs can be periodic in frequency with a uniformity of mode spacing of 7.3×10^{-18} [97]. In fact, mode-locking is not a new idea for WGRs, and has been already explored theoretically for Er:LiNbO₃ WGRs some years ago [98]. Experimental evidence of time resolved pulsed excitation of WGRs exists [99], as well as time resolved monitoring of WGRs [100], but steady pulsed operation in a WGR has been not yet demonstrated. In this work, I coherently excite the eigenmodes of a passive Z-cut LiNbO₃ disk WGR by using a long-cavity mode-locked fiber laser (MDFL) as external excitation. To the best of my knowledge, this is the first report of steady-state pulsed functioning of a WGR, and in a fully fiber optic setup (coupling to the WGR here is in free space, but a fiber-coupled equivalent to my setup has been demonstrated [101]).

The disk was fabricated at the Optoelectronics Circuits and System Laboratory, at the University of California at Los Angeles (UCLA) and has similar characteristics of a disk described elsewhere [102]. The diameter is $d \simeq 5.9$ mm and it has lateral spherical profile, to create an equator along the vertical direction of the disk, hence it behaves a spherical WGR [103]. TE polarized light is coupled by evanescent waves in and out of the WGR using two diamond prisms, whose refractive index $n_o \simeq 2.386$ [104] is larger than the extraordinary index $n_e \simeq 2.138$ of LiNbO₃ [105] in all the spectral region of interest for this work (vacuum wavelength $\lambda \simeq 1550$ nm). Double prism setup is selected because it avoids interference between the output and the uncoupled fraction of the input beam.

Data from CW characterization of the whispering modes of the disk are shown in Fig. 15. The extracted Q -factor is $2.63 \times 10^6 [\pm 12\%]$. The insertion loss between input and output at resonance is 29 dB (the coupling setup with the double prism is not optimized for loss minimization). For coherent pulsed operation, I must match the WGR's FSR — or one of its integer submultiple $1/N$ — with an integer multiple M of the MDFL's fundamental repetition rate. As well known, disk resonators exhibit sets of modes with different FSRs, depending on the radial order of the modes [86,103]. Here, I select the best coupled mode (the highest peak in the transmission spectrum in Fig. 15) for convenience. The extracted FSR of this set of modes, from CW data extending beyond the range shown in Fig. 15, is 7.78 GHz. I then setup an active-locked MLFL with long cavity, in the sense that its fundamental repetition rate $f_R \simeq 2.3$ MHz is much lower than the FSR. A close match $\text{FSR}/N \simeq M \times f_R$ (assuming N small integer) is then

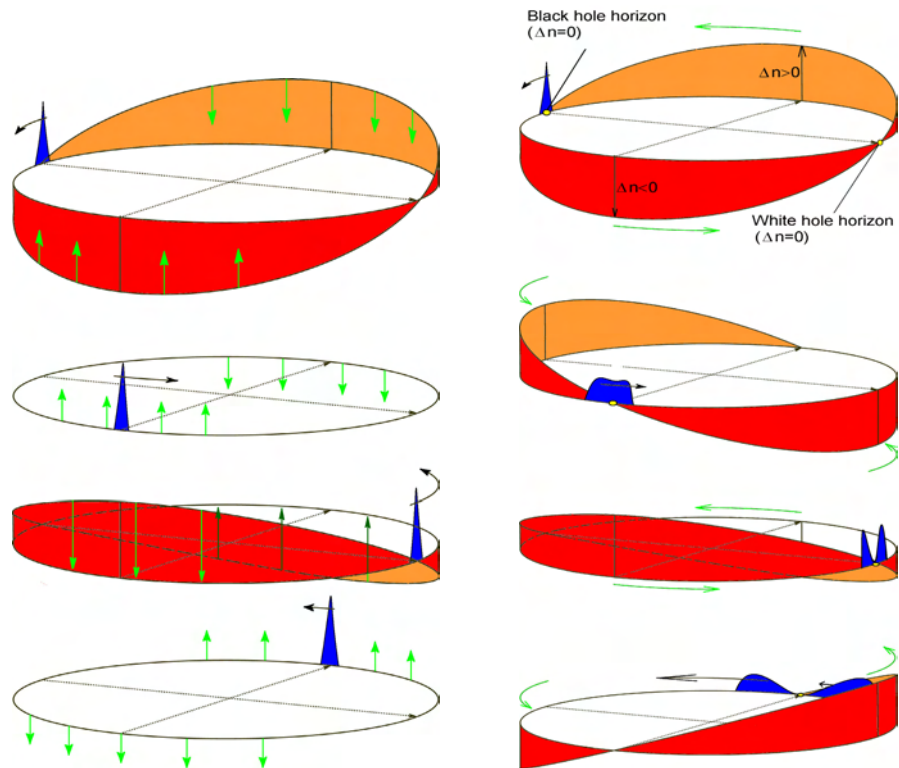


Fig. 14. Left side: the carrier frequency of an optical pulse (envelope shown in blue color), traveling along the equatorial circle of a WGR carved out of a material exhibiting large Pockels effect, can be monotonically shifted. In this example, Pockels effect is driven by a stationary microwave (red-orange: index change due to Pockels effect; green arrows: direction of the index change in time). Monotonic frequency shift is guaranteed if and only if the frequency of the microwave matches the free spectral range of the optical modes. The amount of the shift depends on the ability of keeping the pulse within the WGR (i.e. on the Q-factor). In the NIR, the shift in wavelength can realistically be several tens of nm. Right side: if the index change is driven by a traveling rather than a stationary wave and if the revolution times of the microwave and the optical pulse are the same, then a traveling event horizon is created, at point where the variation of the optical refractive index due to Pockels effect is 0. An optical pulse placed across this point splits, similarly to what expected in presence of a gravitational event horizon. The analogy is further strengthened by the fact that the redshift in time at the event horizon diverges to infinity.

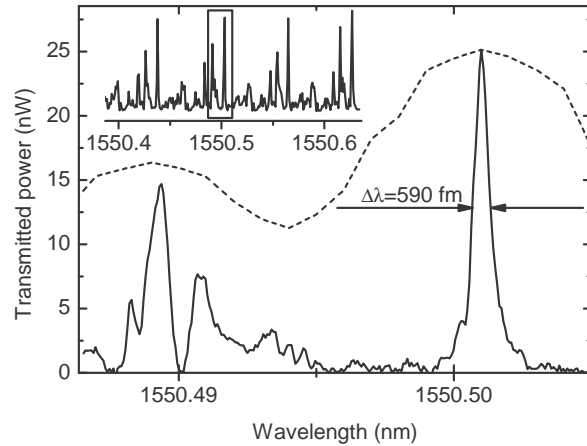


Fig. 15. Transmission spectrum of the LiNbO_3 Whispering Gallery Resonator. The measurement was taken with a CW laser with piezo-tunable cavity (solid lines). Dashed line is acquired with a lower resolution Optical Spectrum Analyzer for absolute wavelength calibration. Inset: larger wavelength span (the portion of main panel is boxed). Input power is $\simeq 20\mu\text{W}$. Extracted Q -factor is $2.63 \times 10^6 [\pm 12\%]$.

possible by a suitable selection of the integer number M , with a resolution equal to the ratio $N \times f_R / \text{FSR}$. From the laser specifications, the injected traveling pulse has a duration of the order of few ps, i.e. significantly shorter than WGR's round trip time $\tau_{rt} = (\text{FSR})^{-1} \simeq 128$ ps. The setup is schematically represented in Fig. 16. I have set the RF source to FSR/N — with

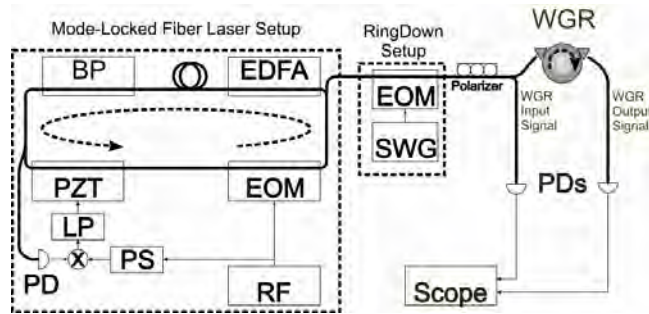


Fig. 16. Schematic representation of the experimental setup. The model locked laser was based on a cavity built as a close optical fiber loop passing through a gain medium (Erbium Doped Fiber Amplifier, EDFA) and a wavelength Band Pass (BP) selecting filter. The pulsed operation was achieved with active mode locking by modulating the cavity loss with an Electro-Optical Modulator (EOM) driven by a RF generator.

$N = 2$ — rather than to FSR. This has the following advantages: (i) since the whispering mode rate is FSR, the observation of the output can be unequivocally attributed to the WGR output, and not to a stray coupling from the input fiber or prism, which would conserve the rate of the input; (ii) this way, I show that the WGR can work as a repetition rate N -multiplier, a fact which can be interesting for example for optical clock distribution; (iii) in the output, I have a sequence of sets of N pulses: each set is composed by a leading pulse, which exit before a complete round trip from the excitation, and $N - 1$ pulses, each completing respectively 1,2,... $N - 1$ additional round trips before the following excitation. The relative difference in intensity between adjacent pulses gives directly the fractional loss F per round trip.

Potentially critical effects for maintaining phase coherence in LiNbO₃ are dispersion, self phase modulation, and temperature dependence of the refractive index. To minimize dispersion, I first consider that pulses with a few ps duration have a spectrum width of the order of 1 nm at wavelength $\lambda \simeq 1550$ nm. The relative refractive index variation $\Delta n_e/n_e$ over 1 nm is of the order of 10^{-5} [105]. The effect on the group velocity

$$v_g = c \left(n - \lambda \frac{dn}{d\lambda} \right)^{-1}, \quad (39)$$

where c is the speed of light in vacuum is of the order of 1% across the spectral components of the pulse. This is in principle enough to introduce a measurable pulse chirp, but I observe no detectable effect in my setup (here, the main limitation with respect to this is the 12 GHz photodetector bandwidth). This point deserves further investigation.

Self phase modulation and temperature dependence of the refractive index ($dn_e/dT = 37 \times 10^{-6}/^\circ C$) [106, 107] depend on light intensity. It is difficult to estimate these effects from principles without knowledge of the spatial distribution of the electric field in the whispering gallery mode. I experimentally look at the dependence of the transmission spectrum on the input power. Resonant wavelengths in a WGR satisfy the approximate condition $\lambda = \pi d n_e / I$ where d is the WGR diameter and I is an integer number [103]. Thus the relative spectrum shifts are approximately equal to the relative changes of the refractive index. I find that the relative variation of the refractive index induced by input power below few hundreds μW is lower than 10^{-6} . Hence, I expect that in such case the effect of intensity is low compared to dispersion. In my experiment, I have limited the input average power to $3.7 \mu W$, with peak power $105 \mu W$. It should be noticed that the difference between average and peak power is not as large as usually found in optical pulses, because the pulse duration is less than 2 orders of magnitudes shorter than the inverse of the MDFL's repetition rate.

The time resolved input and output are shown in Fig. 17 for my case ($N = 2$). The measured

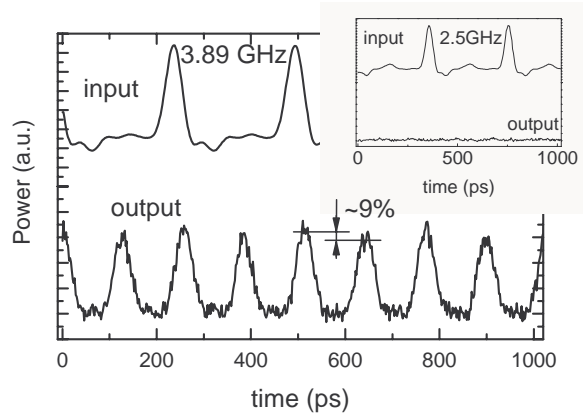


Fig. 17. Steady state input and output optical signals collected by a 12-GHz bandwidth photodetector. The actual duration of optical pulses is of the order of 2 ps, from laser specifications. Output is rescaled for clarity (average power of input and output are, respectively, $3.7 \mu W$ and $1.5 nW$). Inset: example of a mismatched repetition rate, demonstrating no coherent build up.

insertion loss between input and output is 34 dB. Thus, there is an addition 5 dB loss with respect to the CW operation. The discussion of this loss requires the spectral analysis of the signals and is the subject of an upcoming paper.

I estimate from averaging multiple output pulses (the procedure not shown in Fig. 17) a fractional loss $F \simeq 9\%$ per round trip. From

$$Q = \frac{2\pi c}{\lambda FSR \ln(1-F)^{-1}}, \quad (40)$$

where c is the speed of light in vacuum and λ is the carrier wavelength, I estimate a $Q \simeq 1.6 \times 10^6$, which is a consistent estimation within an order of magnitude with respect to the CW value extracted from Fig. 15. No apparent broadening is evident in the output pulses of Fig. 17. While it is not possible to fully exclude that broadening is taking place (due to the limited bandwidth of the detector), the output pulses are the result of steady-state, coherent piling-up of the input periodic excitation, and therefore the absence of detectable broadening is associated to a travel time of several tens of WGR's roundtrips.

For the pulsed ringdown measurement (Fig. 18), the input train is modulated by an electro-optical modulator driven by a low-frequency square wave, with 2 ns risetime. The extracted

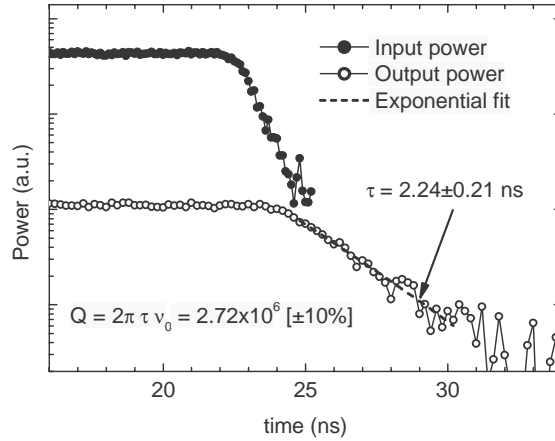


Fig. 18. Pulsed ringdown of the LiNbO₃ whispering gallery resonator. The input and output power are, respectively, the average power of the pulse trains shown in Fig. 17. The output curve has been upshifted for clarity.

Q -factor $2.72 \times 10^6 [\pm 12\%]$ is in excellent agreement with the CW value. This consistency suggests that nonlinear effects and dispersion are not playing a limiting effect in this experiment.

4 CONCLUSIONS

I have proposed several ideas for novel photonic devices to shift the carrier frequency of an optical pulse without affecting its shape nor its coherence, by introducing two complementary principles (Doppler shift and time refraction) and by discussing possible realizations. Finite Difference Time Domain simulations of the proposed dynamic structures have been performed by using a package which has been developed in house to allow time-dependent dielectrics. I have also indicated that the most feasible design appears to be the one relying on a single multimode cavity. In view of such indication, I am now approaching the experimental verification of the lifting idea and of the generation of an event horizon. My preliminary experiments have been so far limited to a pulsed excitation (without any frequency shift) of whispering gallery modes in a LiNbO₃ whispering gallery disk resonator by coupling it to an external actively mode-locked fiber laser, in a full fiber optics setup. Consistent Q -factor measurement has been found between CW and pulsed ringdown characterization.

Acknowledgments

The author acknowledges Prof. Bahram Jalali (UCLA) for fruitful discussions and for providing all the equipment and the samples for this work, with all the members of his group, especially Keisuke Goda, Daniel Solli, Rick Hsu, Dimitri Dimitropoulos, Ali Ayazi, and David Borlaug. Scientific interaction with Prof. Lorenzo Pavesi, the members of Nanoscience Laboratory at the University of Trento (Italy), Francesco Riboli, Iacopo Carusotto, Alessio Recati, Mher Ghulinyan, Claudio Mazzoleni, Leonardo Ricci and third year undergraduate physics students at the University of Trento is also acknowledged. This work was supported in part by the EU-funded FP7 ICT Project WADIMOS.

References

- [1] S. M. Hawking, “Black hole explosion?,” *Nature* **248**, 30-31 (1974) [doi:10.1038/248030a0].
- [2] W. G. Unruh, “Experimental black-hole evaporation?,” *Phys. Rev. Lett.* **46**, 1351-1353 (1981) [doi:10.1103/PhysRevLett.46.1351].
- [3] T. A. Jacobson and G. E. Volovik, “Event horizons and ergoregions in ^3He ,” *Phys. Rev. D* **58**, 064021 (1998) [doi:10.1103/PhysRevD.58.064021].
- [4] L. J. Garay, J. R. Anglin, J. I. Cirac, and P. Zoller, “Sonic analog of gravitational black holes in Bose-Einstein condensates,” *Phys. Rev. Lett.* **85**, 4643 (2000) [doi:10.1103/PhysRevLett.85.4643].
- [5] C. Barceló, S. Liberati, and M. Visser, “Towards the observation of Hawking radiation in Bose-Einstein condensates,” *Int. J. Mod. Phys. A* **18**, 3735 (2003) [doi:10.1142/S0217751X0301615X].
- [6] C. Barceló, S. Liberati, and M. Visser, “Probing semiclassical analog gravity in Bose-Einstein condensates with widely tunable interactions,” *Phys. Rev. A* **68**, 053613 (2003) [doi:10.1103/PhysRevA.68.053613].
- [7] S. Giovanazzi, C. Farrell, T. Kiss, and U. Leonhardt, “Conditions for one-dimensional supersonic flow of quantum gases,” *Phys. Rev. A* **70**, 063602 (2004) [doi:10.1103/PhysRevA.70.063602].
- [8] C. Barceló, S. Liberati, and M. Visser, “Analogue gravity,” *Living Rev. Relat.* **8**, 12 (2005).
- [9] R. Schützhold, “Detection scheme for acoustic quantum radiation in Bose-Einstein condensates,” *Phys. Rev. Lett.* **97**, 190405 (2006) [doi:10.1103/PhysRevLett.97.190405].
- [10] S. Wuester and C. M. Savage, “Limits to the analog Hawking temperature in a Bose-Einstein condensate,” *Phys. Rev. A* **76**, 013608 (2007) [doi:10.1103/PhysRevA.76.013608].
- [11] P. O. Fedichev and U. R. Fischer, “Gibbons-Hawking effect in the sonic de Sitter spacetime of an expanding Bose-Einstein condensed gas,” *Phys. Rev. Lett.* **91**, 240407 (2003) [doi:10.1103/PhysRevLett.91.240407].
- [12] M. Uhlmann, Y. Xu, and R. Schützhold, “Aspects of cosmic inflation in expanding Bose-Einstein condensates,” *New J. Phys.* **7**, 248-264 (2005) [doi:10.1088/1367-2630/7/1/248].
- [13] P. Jain, S. Weinfurter, M. Visser, and C. W. Gardiner, “Analog model of a Friedmann-Robertson-Walker universe in Bose-Einstein condensates: application of the classical field method,” *Phys. Rev. A* **76**, 033616 (2007) [doi:10.1103/PhysRevA.76.033616].
- [14] P. Jain, A. S. Bradley, and C. W. Gardiner, “Quantum de Laval nozzle: stability and quantum dynamics of sonic horizons in a toroidally trapped Bose gas containing a superflow,” *Phys. Rev. A* **76**, 023617 (2007) [doi:10.1103/PhysRevA.76.023617].
- [15] S. Giovanazzi, “Hawking radiation in sonic black holes,” *Phys. Rev. Lett.* **94**, 061302 (2005) [doi:10.1103/PhysRevLett.94.061302].

- [16] U. Leonhardt and P. Piwnicki, “Relativistic effects of light in moving media with extremely low group velocity,” *Phys. Rev. Lett.* **84**, 822-825 (2000) [doi:10.1103/PhysRevLett.84.822].
- [17] W. G. Unruh and R. Schützhold, “On slow light as a black hole analogue,” *Phys. Rev. D* **68**, 024008 (2003) [doi:10.1103/PhysRevD.68.024008].
- [18] R. Schützhold and W. G. Unruh, “Hawking radiation in an electromagnetic waveguide?,” *Phys. Rev. Lett.* **95**, 031301 (2005) [doi:10.1103/PhysRevLett.95.031301].
- [19] E. Yablonovitch, “Accelerating reference frame for electromagnetic waves in a rapidly growing plasma: Unruh-Davies-Fulling-DeWitt radiation and the nonadiabatic Casimir effect,” *Phys. Rev. Lett.* **62**, 1742 - 1745 (1989) [doi:10.1103/PhysRevLett.62.1742].
- [20] E. Yablonovitch, “Black hole radiation: can nonlinear optics produce a similar effect in semiconductors?,” in *Resonances, a Volume in Honor of the 70th Birthday of N. Bloembergen*, M.D. Levenson, E. Mazur, P.S. Pershan, Y.R. Shen (Eds.), World Scientific, Singapore (1990).
- [21] T. G. Philbin, C. Kuklewicz, S. Robertson, S. Hill, F. König, and U. Leonhardt, “Fiber-optical analog of the event horizon,” *Science* **319**, 1367-1370 (2008) [doi:10.1126/science.1153625].
- [22] G. Rousseaux, C. Mathis, P. Maïssa, T. G. Philbin, and U. Leonhardt, “Observation of negative-frequency waves in a water tank: a classical analogue to the Hawking effect?,” *New J. Phys.* **10**, 053015 (2008) [doi:10.1088/1367-2630/10/5/053015].
- [23] C. Yeh, “Reflection and transmission of electromagnetic waves by a moving dielectric medium,” *J. Appl. Phys.* **36**, 3513-3517 (1965) [doi:10.1063/1.1703029].
- [24] C. Yeh and K. F. Casey, “Reflection and transmission of electromagnetic waves by a moving dielectric slab,” *Phys. Rev.* **144**, 665-669 (1966) [doi: 10.1103/PhysRev.144.665].
- [25] T. K. Shiozawa, K. Hazawa, and N. Kumagai, “Reflection and transmission of electromagnetic waves by a dielectric half-space moving perpendicular to the plane of incidence,” *J. Appl. Phys.* **38**, 4459-4461 (1967) [doi:10.1063/1.1709148].
- [26] V. P. Pyati, “Reflection and refraction of electromagnetic waves by a moving dielectric medium,” *J. Appl. Phys.* **38**, 652-655 (1967) [doi:10.1063/1.1709390].
- [27] P. Daly and H. Gruenberg, “Energy relations for plane waves reflected from moving media,” *J. Appl. Phys.* **38**, 4486-4489 (1967) [doi:10.1063/1.1709154].
- [28] J. M. Saca, “Snell’s law for the Poynting vector in a semi-infinite dielectric moving perpendicularly to the surface,” *J. Mod. Opt.* **36**, 1367-1376 (1989) [doi:10.1080/09500348914551401].
- [29] Y.-X. Huang, “Reflection and transmission of electromagnetic waves by a dielectric medium moving in an arbitrary direction,” *J. Appl. Phys.* **76**, 2575-2581 (1994) [doi:10.1063/1.357552].
- [30] F. R. Morgenthaler, “Velocity modulation of electromagnetic waves,” *IEEE Trans. Microwave Theory Tech.* **6**, 167-172 (1958) [doi:10.1109/TMTT.1958.1124533].
- [31] E. Segev, B. Abdo, O. Shtempluck, E. Buks, and B. Yurke, “Prospects of employing superconducting stripline resonators for studying the dynamical Casimir effect experimentally,” *Phys. Lett. A* **370**, 202-206 (2007) [doi:10.1016/j.physleta.2007.05.066].
- [32] F. Biancalana, A. Amann, A. V. Uskov, and E. P. O’Reilly, “Dynamics of light propagation in spatiotemporal dielectric structures,” *Phys. Rev. E* **75**, 046607 (2007) [doi:10.1103/PhysRevE.75.046607].
- [33] S. C. Wilks, J. M. Dawson, and W. B. Mori, “Frequency up-conversion of electromagnetic radiation with use of an overdense plasma,” *Phys. Rev. Lett.* **61**, 337-340 (1988) [doi:10.1103/PhysRevLett.61.337].

- [34] R. L. Savage, Jr., C. Joshi, and W. B. Mori “Frequency upconversion of electromagnetic radiation upon transmission into an ionization front,” *Phys. Rev. Lett.* **68**, 946-949 (1992) [doi:10.1103/PhysRevLett.68.946].
- [35] A. S. Pirozhkov, J. Ma, M. Kando, T. Z. Esirkepov, Y. Fukuda, L.-M. Chen, I. Daito, K. Ogura, T. Homma, Y. Hayashi, H. Kotaki, A. Sagisaka, M. Mori, J. K. Koga, T. Kawachi, H. Daido, S. V. Bulanov, T. Kimura, Y. Kato, and T. Tajima, “Frequency multiplication of light back-reflected from a relativistic wake wave,” *Phys. Plasmas* **14**, 123106 (2007) [doi:10.1063/1.2816443].
- [36] O. Boyraz and B. Jalali, “Demonstration of a silicon Raman laser,” *Opt. Exp.* **12**, 5269-5273 (2004) [doi:10.1364/OPEX.12.005269].
- [37] H. Rong, A. Liu, R. Jones, O. Cohen, D. Hak, R. Nicolaescu, A. Fang, and M. Paniccia, “An all-silicon Raman laser,” *Nature* **433**, 292-294 (2005) [doi:10.1038/nature03273].
- [38] H. Rong, R. Jones, A. Liu, O. Cohen, D. Hak, A. Fang, and M. Paniccia, “A continuous-wave Raman silicon laser,” *Nature* **433**, 725-728 (2005) [doi:10.1038/nature03346].
- [39] E. J. Reed, M. Soljačić, and J. D. Joannopoulos, “Color of shock waves in photonic crystals,” *Phys. Rev. Lett.* **90**, 203904 (2003) [doi:10.1103/PhysRevLett.90.203904].
- [40] C. Thaury, F. Quéré, J.-P. Geindre, A. Levy, T. Ceccotti, P. Monot, M. Bougeard, F. Réau, P. d’Oliveira, P. Audebert, R. Marjoribanks, and Ph. Martin, “Plasma mirrors for ultrahigh-intensity optics,” *Nature Phys.* **3**, 424-429 (2007) [doi:10.1038/nphys595].
- [41] B. A. Auld, J. H. Collins, and H. R. Zapp, “Signal processing in a nonperiodically time-varying magnetoelastic medium,” *Proc. IEEE* **56**, 258-272 (1968) [doi:10.1109/PROC.1968.6270].
- [42] B. L. Felsen and G. M. Whitman, “Wave propagation in time-varying media,” *IEEE Trans. Antennas Propag.* **18** 242-253 (1970) [doi:10.1109/TAP.1970.1139657].
- [43] R. L. Fante, “Transmission of electromagnetic waves into time-varying media,” *IEEE Trans. Antennas Propag.* **19**, 417-424 (1971) [doi:10.1109/TAP.1971.1139931].
- [44] E. Yablonovitch, “Spectral broadening in the light transmitted through a rapidly growing plasma,” *Phys. Rev. Lett.* **31**, 877-879 (1973) [doi:10.1103/PhysRevLett.31.877].
- [45] C. L. Jiang, “Wave propagation and dipole radiation in a suddenly created plasma,” *IEEE Trans. Antennas Propag.* **23**, 83-90 (1975) [doi:10.1109/TAP.1975.1141007].
- [46] M. Lampe and J. H. Walker, “Interaction of electromagnetic waves with a moving ionization front,” *Phys. Fluids* **21**, 42-54 (1978) [doi:10.1063/1.862069].
- [47] J. C. AuYeung, “Phase-conjugate reflection from a temporal dielectric boundary,” *Opt. Lett.* **8** 148-150 (1983). [doi:10.1364/OL.8.000148].
- [48] D. K. Kalluri, “Effect of switching a magnetoplasma medium on a travelling wave: Longitudinal propagation,” *IEEE Trans. Antennas Propag.* **37** 1638-1642 (1989) [doi:10.1109/8.451111].
- [49] C. J. Joshi, C. E. Clayton, K. Marsh, D. B. Hopkins, A. Sessler, and D. Whittum, “Demonstration of the frequency upshifting of microwave radiation by rapid plasma creation,” *IEEE Trans. Plasma Sci.* **18**, 814-818 (1990) [doi:10.1109/27.62347].
- [50] S. P. Kuo, “Frequency up-conversion of microwave pulse in a rapidly growing plasma,” *Phys. Rev. Lett.* **65**, 1000-1003 (1990) [doi:10.1103/PhysRevLett.65.1000].
- [51] M. Rader, F. Dyer, A. Matas, and I. Alexeff, “Plasma-induced frequency shifts in microwave beams,” in *Proc. IEEE Int. Conf. Plasma Sci.*, Oakland, CA, p. 171 (1990) [doi:10.1109/PLASMA.1990.110740].
- [52] S. P. Kuo and A. Ren, “Experimental study of wave propagation through a rapidly created plasma,” *IEEE Trans. Plasma Sci.* **21** 5356 (1993) [doi:10.1109/27.221101].
- [53] A. Banos, Jr., W. B. Mori, and J. M. Dawson, “Computation of the electric and magnetic fields induced in a plasma created by ionization lasting a finite interval of time,” *IEEE Trans. Plasma Sci.* **21**, 5769 (1993) [doi:10.1109/27.221102].

- [54] D. K. Kalluri, *Electromagnetics of Complex Media*, CRC Press, Boca Raton, FL (1999).
- [55] S. P. Kuo, D. Bivolaru, L. Orlick, I. Alexeff, and D. K. Kalluri, "A transmission line filled with fast switched periodic plasma as a wideband frequency transformer," *IEEE Trans. Plasma Sci.* **29** 365-370 (2001) [doi:10.1109/27.922747].
- [56] J. T. Mendonça and P. K. Shukla, "Time refraction and time reflection: two basic concepts," *Phys. Scr.* **65**, 160-163 (2002) [doi: 10.1238/Physica.Regular.065a00160].
- [57] J. T. Mendonça and A. Guerreiro, "Time refraction and the quantum properties of vacuum," *Phys. Rev. A* **72**, 063805 (2005) [doi: 10.1103/PhysRevA.72.063805].
- [58] A. Degiron, J. J. Mock, and D. R. Smith, "Modulating and tuning the response of metamaterials at the unit cell level," *Opt. Exp.* **15**, 1115-1127 (2007) [doi:10.1364/OE.15.001115].
- [59] H.-T. Chen, W. J. Padilla, J. M. O. Zide, S. R. Bank, A. C. Gossard, A. J. Taylor, and R. D. Averitt, "Ultrafast optical switching of terahertz metamaterials fabricated on ErAs/GaAs nanoisland superlattices," *Opt. Lett.* **32**, 1620-1622 (2007) [doi:10.1364/OL.32.001620].
- [60] H.-T. Chen, W. J. Padilla, R. D. Averitt, A. C. Gossard, C. Highstrete, M. Lee, J. F. OHara, and A. J. Taylor, "Electromagnetic metamaterials for terahertz applications," *Terahertz Sci. Technol.* **1**, 42-50 (2008).
- [61] S. J. Orfanidis, *Electromagnetic Waves and Antennas*, Rutgers University Press, Piscataway, NJ (2004).
- [62] W. Greiner, *Classical Electrodynamics*, Springer, Berlin (1998).
- [63] A. Sommerfeld, *Electrodynamics*, Academic Press, New York (1952).
- [64] J. D. Jackson, *Classical Electrodynamics*, Wiley, New York (1962).
- [65] A. Gjurchinovski and A. Skeparovski, "Fermat's principle of least time in the presence of uniformly moving boundaries and media," *Eur. J. Phys.* **28**, 933-951 (2007) [doi:10.1088/0143-0807/28/5/017].
- [66] J. Qi Shen, "A note: the relativistic transformations of the optical constants of media," (2004), <http://arxiv.org/abs/physics/0408005v1>.
- [67] M. F. Yanik and S. Fan, "Dynamic photonic structures: stopping, storage and time reversal of light," *Stud. in Appl. Math.* **115**, 233-253 (2005) [doi:10.1111/j.1467-9590.2005.00327.x].
- [68] M. F. Yanik, W. Suh, Z. Wang, and S. Fan, "Stopping light in a waveguide with an all-optical analog of electromagnetically induced transparency," *Phys. Rev. Lett.* **93**, 233903 (2004) [doi:10.1103/PhysRevLett.93.233903].
- [69] M. F. Yanik and S. Fan, "Stopping and storing light coherently," *Phys. Rev. A* **71**, 013803 (2005) [doi:10.1103/PhysRevA.71.013803].
- [70] M. L. Povinelli, S. G. Johnson, and J. D. Joannopoulos, "Slow-light, band-edge waveguides for tunable time delays," *Opt. Exp.* **13**, 7145-7159 (2005) [doi:10.1364/OPEX.13.007145].
- [71] K. J. Vahala, "Optical microcavities," *Nature* **424**, 839 (2003) [doi:10.1038/nature01939].
- [72] B. S. Song, S. Noda, T. Asano, and Y. Akahane, "Ultra-high-Q photonic double-heterostructure nanocavity," *Nature Mater.* **4**, 207 (2005) [doi:10.1038/nmat1320].
- [73] H. Gersen, T. J. Karle, R. J. P. Engelen, W. Bogaerts, J. P. Korterik, N. F. van Hulst, T. F. Krauss, and L. Kuipers, "Real-space observation of ultraslow light in photonic crystal waveguides," *Phys. Rev. Lett.* **94**, 073903 (2005) [doi:10.1103/PhysRevLett.94.073903].
- [74] A. Melloni, F. Morichetti, and M. Martinelli, "Linear and nonlinear pulse propagation in coupled resonator slow-wave optical structures," *Opt. Quantum Electron.* **35**, 365-379 (2003) [doi:10.1023/A:1022957319379].

- [75] J. Scheuer, G.T. Paloczi, J.K.S. Poon and A. Yariv, "Coupled resonator optical waveguides: toward the slowing & storage of light," *OSA Opt. Photon. News* **16** (2), 36-40 (2005) [doi:10.1364/OPN.16.2.000036].
- [76] H. Altug and J. Vučković, "Experimental demonstration of the slow group velocity of light in two-dimensional coupled photonic crystal microcavity arrays," *Appl. Phys. Lett.* **86**, 111102 (2005) [doi:10.1063/1.1882755].
- [77] M. Ghulinyan, C. J. Oton, G. Bonetti, Z. Gaburro, and L. Pavesi, "Free-standing porous silicon single and multiple optical cavities," *J. Appl. Phys.* **93**, 9724-9729 (2003) [doi:10.1063/1.1578170].
- [78] A. Melloni, F. Morichetti and M. Martinelli, "Linear and nonlinear propagation in coupled resonator slow-wave optical structures," *Opt. Quantum Electron.* **35** 365-379 (2003) [doi:10.1023/A:1022957319379].
- [79] A. Galindo and P. Pascual, *Quantum Mechanics II*, Springer, Berlin (1991).
- [80] B. R. Bennett, R. A. Soref, and J. A. Del Alamo, "Carrier-induced change in refractive index of InP, GaAs, and InGaAsP," *IEEE J. Quantum Electron.* **26**, 113-122 (1990) [doi:10.1109/3.44924].
- [81] A. Liu, R. Jones, L. Liao, D. Samara-Rubio, D. Rubin, O. Cohen, R. Nicolaescu, and M. Paniccia, "A high-speed silicon optical modulator based on a metal-oxide-semiconductor capacitor," *Nature* **427**, 615-618 (2004) [doi:10.1038/nature02310].
- [82] Y.-H. Ye, J. Ding, D.-Y. Jeong, I. C. Khoo, and Q. M. Zhang, "Finite-size effect on one-dimensional coupled-resonator optical waveguides," *Phys. Rev. E* **69**, 056604 (2004) [doi:10.1103/PhysRevE.69.056604].
- [83] see, e.g. C. R. Pollock, *Fundamentals of Optoelectronics*, Irwin, Chicago (1995).
- [84] A. S. Sudbo, "Numerically stable formulation of the transverse resonance method for vector mode-field calculations in dielectric waveguides," *IEEE Photon. Technol. Lett.* **5**, 342-344 (1993) [doi:10.1109/68.205632].
- [85] R. C. Alferness, "Optical guided-wave devices," *Science* **234**, 825-829 (1986) [doi:10.1126/science.234.4778.825].
- [86] A. B. Matsko and V. S. Ilchenko, "Optical resonators with whispering-gallery modes Part I: Basics," *IEEE J. Sel. Top. Quantum Electron.* **12**, 3-14 (2006) [doi:10.1109/JSTQE.2005.862952].
- [87] V. S. Ilchenko and A. B. Matsko, "Optical resonators with whispering-gallery modes Part II: Applications," *IEEE J. Sel. Top. Quantum Electron.* **12**, 15-32 (2006) [doi:10.1109/JSTQE.2005.862943].
- [88] M. C. Stowe, M. J. Thorpe, A. Pe'er, J. Ye, J. E. Stalnaker, V. Gerginov, and S. A. Diddams, "Direct frequency comb spectroscopy," *Adv. AMO Phys.* **55**, 1-60 (2008). [doi:10.1016/S1049-250X(07)55001-9]
- [89] R. W. P. Drever, J. L. Hall, F. V. Kowalski, J. Hough, G. M. Ford, A. J. Munley, and H. Ward, "Laser phase and frequency stabilization using an optical resonator," *Appl. Phys. B* **31**, 97105 (1983) [doi:10.1007/BF00702605].
- [90] D. A. B. Miller, A. Bhatnagar, S. Palermo, A. Emami-Neyestanak, and M. A. Horowitz, "Opportunities for optics in integrated circuits applications," *Solid-State Circuits Conference, Digest of Technical Papers ISSCC IEEE International* **1**, 86-87 (2005) [doi:10.1109/ISSCC.2005.1493881]
- [91] M. J. Thorpe, K. D. Moll, R. J. Jones, B. Safdi, and J. Ye, "Broadband cavity ring-down spectroscopy for sensitive and rapid molecular detection," *Science* **311**, 1595-1599 (2006) [doi:10.1126/science.1123921].
- [92] S. Arnold, M. Khoshshima, I. Teraoka, S. Holler, and F. Vollmer, "Shift of whispering-gallery modes in microspheres by protein adsorption," *Opt. Lett.* **27**, 272-274 (2003) [doi:10.1364/OL.28.000272].

- [93] A. M. Armani, R. P. Kulkarni, S. E. Fraser, R. C. Flagan, and K. J. Vahala, "Label-free, single-molecule detection with optical microcavities," *Science* **317**, 783-787 (2007) [doi:10.1126/science.1145002].
- [94] D. Erickson, S. Mandal, A. H. J. Yang, and B. Cordovez, "Nanobiosensors: optofluidic, electrical and mechanical approaches to biomolecular detection at the nanoscale," *Microfluid. Nanofluid.* **4**, 33-52 (2008) [doi:10.1007/s10404-007-0198-8].
- [95] A. A. Savchenkov, A. B. Matsko, V. S. Ilchenko, and L. Maleki, "Optical resonators with ten million finesse," *Opt. Exp.* **15**, 6768-6773 (2007) [doi:10.1364/OE.15.006768].
- [96] U. Keller, "Recent developments in compact ultrafast lasers," *Nature* **424**, 831-838 (2003) [doi:10.1038/nature01938].
- [97] P. DelHaye, A. Schliesser, O. Arcizet, T. Wilken, R. Holzwarth, and T. J. Kippenberg, "Optical frequency comb generation from a monolithic microresonator," *Nature* **450**, 1214-1217 (2007) [doi:10.1038/nature06401].
- [98] A. B. Matsko, V. S. Ilchenko, A. A. Savchenkov, and L. Maleki, "Active mode locking with whispering-gallery modes," *J. Opt. Soc. Am. B* **20**, 2292-2296 (2003) [doi:10.1364/JOSAB.20.002292].
- [99] R. W. Shaw, W. B. Whitten, M. D. Barnes, and J. M. Ramsey, "Time-domain observation of optical pulse propagation in whispering-gallery modes of glass spheres," *Opt. Lett.* **23**, 1301-1303 (1998) [doi:10.1364/OL.23.001301].
- [100] H. Gersen, D. J. W. Klunder, J. P. Korterik, A. Driessen, N. F. van Hulst, and L. Kuipers, "Propagation of a femtosecond pulse in a microresonator visualized in time," *Opt. Lett.* **29**, 1291-1293 (2004) [doi:10.1364/OL.29.001291].
- [101] V. S. Ilchenko, X. S. Yao, and L. Maleki, "Pigtailing the high-Q microsphere cavity: a simple fiber coupler for optical whispering-gallery modes," *Opt. Lett.* **24**, 723-725 (1999) [doi:10.1364/OL.24.000723].
- [102] R. C. J. Hsu, A. Ayazi, B. Houshmand and B. Jalali, "All-dielectric photonic-assisted radio front-end technology," *Nature Photon.* **1**, 535-538 (2007) [doi:10.1038/nphoton.2007.145].
- [103] B. E. Little, J.-P. Laine, and H. A. Haus, "Analytic theory of coupling from tapered fibers and half-blocks into microsphere resonators," *J. Lightwave Technol.* **17**, 704-715 (1999) [doi:10.1109/50.754802].
- [104] F. Peter, "Über Brechungsindizes und Absorptionskonstanten des Diamanten zwischen 644 und 226 μm ," *Z. Phys. A* **15**, 358-368 (1923) [doi:10.1007/BF01330487].
- [105] D. F. Nelson and R. M. Mikulyak, "Refractive indices of congruently melting lithium niobate," *J. Appl. Phys.* **45**, 3688-3689 (1974) [doi:10.1063/1.1663839].
- [106] D. S. Smith, H. D. Riccius and R. P. Edwin, "Refractive indices of lithium niobate," *Optic. Comm.* **17** 332-335 (1976) [doi:10.1016/0030-4018(76)90273-X].
- [107] S. D. Smith, H. D. Riccius, and R. P. Edwin, "Errata: Refractive indices of lithium niobate," *Optic. Comm.* **20**, 188 (1977) [doi:10.1016/0030-4018(77)90191-2].